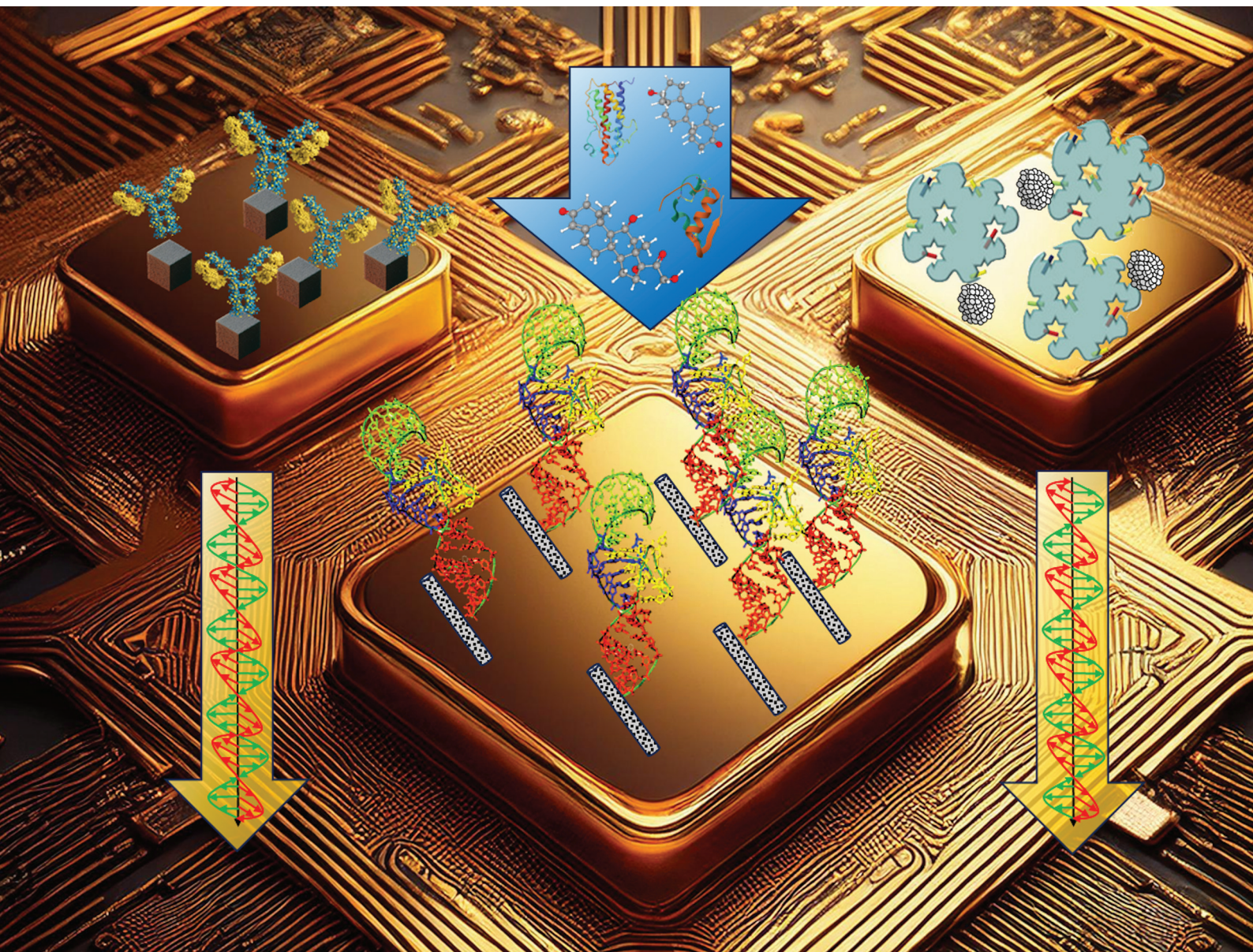


# Nanoscale

rsc.li/nanoscale



ISSN 2040-3372

**REVIEW ARTICLE**

Nguyen Thi Kim Thanh, Riccarda Antiochia *et al.*  
Progress in nanoparticle-based electrochemical biosensors  
for hormone detection



Cite this: *Nanoscale*, 2024, **16**, 18134

# Progress in nanoparticle-based electrochemical biosensors for hormone detection

Francesco Rossi,<sup>a</sup> Thithawat Trakoolwilaiwan,<sup>b,c,d</sup> Valeria Gigli,<sup>e</sup>  
 Cristina Tortolini,<sup>e</sup> Andrea Lenzi,<sup>e</sup> Andrea Maria Isidori,<sup>e</sup>  
 Nguyen Thi Kim Thanh<sup>\*c,d</sup> and Riccarda Antiochia<sup>\*f</sup>

Hormones are chemical messengers that regulate a wide range of physiological processes including metabolism, development, growth, reproduction and mood. The concentration of hormones that orchestrate the numerous bodily functions is very low (1 nM or less). Efforts have been made to develop highly sensitive tools to detect them. This review represents a critical comparison between different types of nanoparticle-based electrochemical biosensors for the detection of various hormones, namely cortisol, sex hormones (estradiol, progesterone, testosterone), insulin, thyroid-stimulating hormone (TSH) and growth hormone (GH). The electrochemical biosensors investigated for each hormone are first divided on the basis of the biological fluid tested for their detection, and successively on the basis of the electrochemical transducer utilized in the device (voltammetric or impedimetric). Focus is placed on the nanoparticles employed and the successive electrode modification developed in order to improve detection sensitivity and specificity and biosensor stability. Limit of detection (LOD), linear range, reproducibility and possibility of regeneration for continuous reuse are also investigated and compared. The review also addresses the recent trends in the development of wearable biosensors and point-of-care testing for hormone detection in clinical diagnostics useful for endocrinology research, and the future perspectives regarding the integration of nanomaterials, microfluidics, near field communication (NFC) technology and portable devices.

Received 15th May 2024,  
 Accepted 16th August 2024  
 DOI: 10.1039/d4nr02075h  
[rsc.li/nanoscale](https://rsc.li/nanoscale)

## 1. Introduction

### 1.1 The role played by hormones in pathology and diagnosis

Hormones are signalling molecules transported to distal organs to regulate various physiological and behavioural functions.<sup>1</sup> Hormones are secreted by glands or specific cells, circulate in the bloodstream, and specialize in targeting certain cells. Knowledge of precise hormone levels, which fluctuate in the human body, is of extreme importance in better understanding the role they play and the potential impact of their imbalance on health and well-being. Levels of hormones are therefore significant diagnostic indicators for possible disease status.

They can be categorized into three systems, namely, steroids, peptides, and amino acid-derived, depending on their building units, as shown in Fig. 1. Steroid hormones possess lipid solubility which enables them to traverse the plasma membranes of target cells and exert their effects within the nuclei. Peptide hormones are composed of amino acid chains, are therefore water-soluble and exert their primary physiological effects on the endocrine system by binding to cell surface receptors.<sup>2–6</sup> Some of them are glycoproteins (TSH, luteinizing hormone, LH, and follicle-stimulating hormone, FSH). Amino acid-derived hormones are small molecules with chemical structures similar to particular amino acids, namely tyrosine (catecholamines) and tryptophan (thyroid hormones).

In this review, we describe the most relevant works published in recent years about electrochemical nanoparticle-based biosensors for the detection of the above-described hormones.

For each of them, a first division has been made according to the biological body fluid of detection, and a sub-classification was further carried out depending on the electrochemical technique employed in each sensing device.

Different voltammetric techniques, namely cyclic voltammetry (CV), differential pulse voltammetry (DPV), square wave voltammetry (SWV) and amperometry, have been indicated with the general term “voltammetric” biosensors in order to

<sup>a</sup>ICCOM-CNR, Polo Scientifico, Via Madonna del piano 10, Sesto Fiorentino, FI, 50019, Italy

<sup>b</sup>Biophysics Group, Department of Physics and Astronomy, University College London, Gower Street, London WC1E 6BT, UK

<sup>c</sup>UCL Healthcare Biomagnetics and Nanomaterials Laboratories, 21 Albemarle Street, London W1S 4BS, UK. E-mail: [ntk.thanh@ucl.ac.uk](mailto:ntk.thanh@ucl.ac.uk)

<sup>d</sup>National Nanotechnology Center (NANOTEC), National Science and Technology Development Agency (NSTDA), Pathum Thani, Thailand

<sup>e</sup>Department of Experimental Medicine, Sapienza University of Rome, Rome, Italy

<sup>f</sup>Department of Chemistry and Drug Technologies, Sapienza University of Rome, Rome, Italy. E-mail: [riccarda.antiochia@uniroma1.it](mailto:riccarda.antiochia@uniroma1.it)



distinguish them from those based on the electrochemical impedance spectroscopy (EIS) technique and referred to as “impedimetric” biosensors.<sup>7–10</sup> Moreover, wearable non-invasive biosensors for hormone detection in biofluids such as sweat and interstitial fluid (ISF) have been reported and discussed. Finally, the review has been concluded with challenges and future perspectives for nanoparticle-based biosensors to detect hormones in various human biofluids.

## 1.2 Relevant hormones and current detection methods

Scientists have identified over 50 hormones in the human body so far. In this review we focus on 7 key hormones which mostly affect the health in our bodies; in particular, 4 lipid hormones derived from cholesterol, *i.e.* cortisol, estradiol, progesterone and testosterone, and 3 peptide hormones, *i.e.* insulin, GH and TSH.

Table 1 displays the different concentrations of primary hormones found in biological fluids, including serum, urine and saliva.<sup>11–22</sup>

**1.2.1 Cortisol.** Cortisol (11 $\beta$ ,17 $\alpha$ ,21-trihydroxypregn-4-ene-3,20-dione) is a steroid hormone synthesized by the zona fasciculata of the adrenal cortex. The release of cortisol is regulated by the hypothalamic–pituitary–adrenal (HPA) axis response, which is the main stress response system of the human body.

The process which leads to the release of cortisol from the adrenal cortex begins in the hypothalamus with the production of corticotropin-releasing factor (CRF). CRF interacts with specific receptors in the pituitary gland and causes the release of adrenocorticotrophic hormone (ACTH), which signals to the adrenal gland cortex to release cortisol into the bloodstream from which it can diffuse to target tissues (Fig. 2).<sup>23</sup>

Cortisol is a small molecule (362.46 g mol<sup>−1</sup>) of neutral electrostatic charge and is soluble in fat. It can pass across cytoplasmic membranes and act as messenger in several metabolic pathways. Because cortisol is released by the organism in response to stress, it regulates several pathways aimed to prepare the body to overcome the crisis. Cortisol is involved in the formation of glucose and its metabolism. At the same time, it is involved in the regulation of appetite, and the concentration of cortisol determines the formation of carbohydrate, proteins or fat.<sup>24</sup> Furthermore, after a bleeding wound, cortisol regulates the activation of anti-inflammatory and anti-stress pathways.<sup>25</sup>

Persistently high levels of cortisol can lead to serious health conditions such as insulin resistance, dyslipidaemia, hypertension and obesity. Longer exposure to high cortisol concentrations can lead to bone demineralization, difficulties in the intestinal absorption of calcium, water retention and muscle breakdown.<sup>23,24</sup> The involvement of cortisol in numerous stress-related diseases and conditions makes it a prime diagnostic target for the detection of persistent stress levels and for preventing related conditions.<sup>26</sup> In the absence of any pathology, cortisol levels change during the day in a reproducible cycle, peaking in the morning approximately one hour after waking up and progressively decreasing to reach a minimum around midnight.<sup>27</sup>

Because cortisol is able to pass cytoplasmic membranes it can be found in detectable concentrations in many parts of the human body; the most relevant for its detection are hair, saliva, sweat, urine, blood, and interstitial fluid.<sup>28–34</sup>

In an analytical laboratory setting, cortisol quantification is obtained using three main techniques: liquid chromatography



**Francesco Rossi**

*Dr Francesco Rossi received a BSc in Chemistry (2011) and MSc in Nanotechnology (2013) at the University of Florence (Italy). In 2020 he received a PhD in Biophysics and Nanotechnology from University College London (UCL), London (United Kingdom). Between 2021 and 2022 he held the position of lecturer of Chemistry for the international students of Ca'Foscari University (Venice, Italy). Since February 2024 he*

*has been a postdoctoral researcher at the Institute for the Chemistry of Organometallic Compounds (ICCOM) of the Consiglio Nazionale delle Ricerche (CNR, Italy). His research is focused on the application of nanomaterials to different fields of everyday life, from nanomedicine to self-sterilizing surfaces. Recently he has been collaborating with the CNR to develop ligands for multi-center magnetic complexes for advanced computing.*



**Thithawat Trakoolwilaiwan**

*Dr Thithawat Trakoolwilaiwan earned his bachelor's degree with first-class honours from Mahidol University, majoring in biomedical engineering. Following his graduation, he was awarded a Royal Thai Government scholarship to pursue further studies in the UK. He studied biomaterials and tissue engineering, earning a distinction in his master's degree from University College London. Subsequently, he did a PhD in*

*Biophysics at the same institution, under the supervision of Professor Nguyen T. K. Thanh. His doctoral research focused on the development of a photothermal-based lateral flow assay. Currently, he is working at the National Nanotechnology Center in Thailand, where his work is dedicated to developing nanotechnology for advancements in food and agricultural applications.*



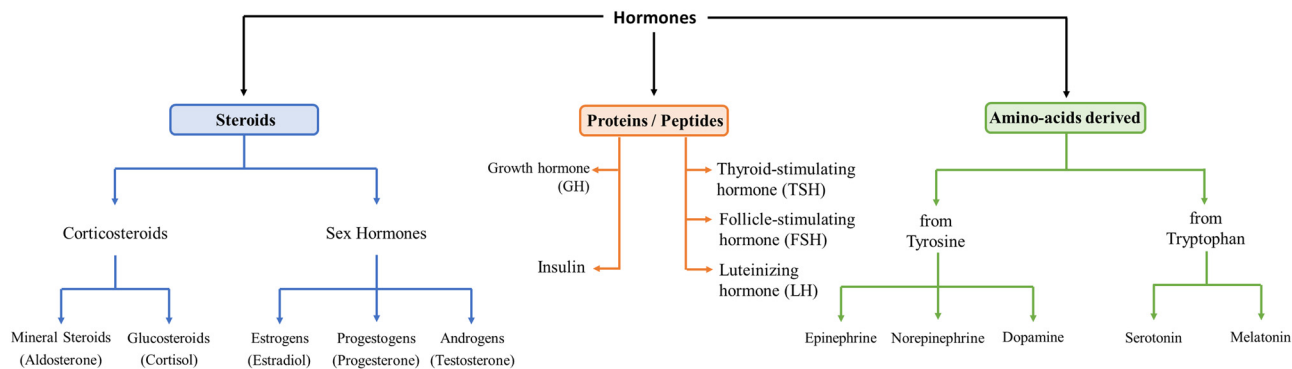


Fig. 1 Classification of hormones based on their building units.

paired with tandem mass spectroscopy/mass spectroscopy (LC-MS/MS), radioimmunoassay (RIA) and enzyme-linked immunoassay (ELISA).<sup>27</sup> LC-MS/MS is mostly used for quantitative analysis, because it has a low LOD of  $0.1 \text{ ng mL}^{-1}$  and it can test samples in a wide range of concentrations, but it requires sophisticated equipment and trained personnel.<sup>35</sup>

Commercial RIA kits have a LOD of  $8.6 \text{ nM}$  and they are easier to perform. But a great limitation to their use is the need for radioisotopes to use as markers, which produces dangerous waste that is difficult to dispose of.<sup>36</sup> ELISA immunoassays are the most recent and commonly used technique; they have good selectivity for cortisol compared with other steroids, but their accuracy and reproducibility is still lacking compared with LC-MS/MS.<sup>37,38</sup> All three of these techniques are expensive to run (LC-MS/MS, RIA), require specialized personnel and waste management (LC-MS/MS, RIA) and are time consuming (ELISA 1.5–2 h).

Electrochemical measurements have several advantages compared with the above techniques: they are usually simpler to use than LC-MS/MS, they do not require toxic or radioactive material as does RIA, they do not need to destroy the sample as does the ELISA, and they are usually faster with no direct intervention required by an operator. It is interesting to note that these advantages are valid for the detection of all hormones and not only for cortisol detection. On the other hand, they offer some unique advantages; for example, an electrochemical cortisol detector can be deployed to the point of care (PoC), they have a limit of detection and selectivity similar to ELISA and can track the cortisol level during the day.<sup>23,26,39</sup>

**1.2.2 Sex hormones.** Sex hormones are steroid hormones derived from cholesterol which play a crucial role in regulating both reproductive and non-reproductive systems, influencing sexual function and behavior. They serve as chemical messen-



Valeria Gigli

Valeria Gigli obtained her biotechnology degree and the equivalent research master degree in industrial biotechnology from the Department of Innovation in Biological, Agri-Food and Forestry Systems of the University of Tuscia, Italy, in 2021. Currently, she is doing a PhD at the Sapienza University of Rome (Italy) in the Department of Experimental Medicine under the supervision of Professor Riccarda Antiochia.

During her PhD studies, she embarked on a visiting PhD program at University College London, focusing on synthesizing cutting-edge metallic nanomaterials for biomedical applications. She worked under the guidance of Professor T. K. Thanh during this tenure. Her ongoing research initiatives revolve around the design and advancement of electrochemical biosensors tailored for monitoring hormones and their metabolites.



Cristina Tortolini

Dr Cristina Tortolini received her PhD degree in Chemical Sciences from the Sapienza University of Rome in 2015. Then she worked as a post-doc in the Department of Chemistry and Drug Technologies of Sapienza and her activity involved the development, characterization and application of biosensors/immunosensors modified by different nanomaterials in the analytical field.

Currently, her research at the Department of Experimental Medicine of Sapienza focuses on electrochemical platforms for the detection of analytes of clinical interest.



gers in the body, and their actions are mediated by receptors within various central nervous system structures, including the hypothalamus, midbrain, amygdala, cortex, and pituitary gland. Binding to specific receptors, sex hormones elicit cellular responses through both genomic and non-genomic mechanisms, involving signal transduction processes.<sup>40,41</sup>

Sex hormones are vital for sexual development and function in both males and females, each eliciting unique effects. While androgens are commonly referred to as male sex hormones due to their masculinizing effects, estrogens and progestogens are considered female hormones. It's crucial to note that all sex hormones are present in each gender, contributing to various functions across organs and systems.<sup>42–47</sup>

Estrogen is present in both blood and interstitial fluid. Upon binding, estrogen permeates the cell membrane, entering the cell nucleus and forming a hormone–receptor structure. This structure, known as a dimer, binds to specific sequences in the genome called estrogen-response elements situated in regions that regulate gene transcription. Estrogen acts through various nuclear receptors, influencing tissues such as the endometrium, vagina, and breast. Its non-genomic activities include the removal of granular calcium cells and modulation of uterine blood flow, occurring independently of cellular receptors. Additionally, estrogens counteract the effects of parathyroid hormone, minimizing calcium loss from bones and promoting bone strength. Estrogens find applications in hormone replacement therapy for menopause, oncology, and contraceptives. In summary, estrogens play a crucial role in developing and maintaining both internal and external genitalia, enhancing skin appearance and functionality, improving bone density through increased osteoblastic activity, regulating kidney retention of sodium, chloride, and water, and reducing overall cholesterol levels in the body.<sup>48–54</sup>

Progesterone, secreted by the corpus luteum and placenta, plays pivotal roles in both the menstrual cycle and pregnancy. Its applications extend to hormonal contraception, long-term ovarian suppression in conditions like dysmenorrhea, endome-

triosis, hirsutism, and bleeding disorders. Often combined with estrogen to mitigate uterine or cervical cancer risk, progesterone is integral to hormone replacement therapy and feminizing hormone therapy. In addition to its essential functions, progesterone serves as a crucial metabolic intermediate along the production pathways for various endogenous steroids, encompassing sex hormones, corticosteroids, and neurosteroids. Its effects are amplified in the presence of estrogen, with estrogen receptors upregulating or inducing the extraction of progesterone receptors. An imbalance in progesterone levels impacts aldosterone function, influencing sodium retention and extracellular fluid volume. In the reproductive system, progesterone engages in non-genomic signaling affecting sperm, modulating intracellular calcium signaling and sperm motility. During pregnancy, progesterone contributes to endometrial preparation for implantation, thickening vaginal epithelium, making cervical mucus impenetrable to sperm, and inhibiting lactation. In the absence of pregnancy, declining progesterone facilitates menstruation, considered a consequence of progesterone withdrawal. Beyond reproduction, progesterone plays a role in breast development and is implicated in breast cancer pathophysiology. Similar to estrogen, it influences skin health, with decreased levels during menopause contributing to skin atrophy and increased wrinkling. Hormone replacement therapy, including progesterone, enhances skin characteristics such as collagen content, thickness, elasticity, hydration, and surface lipids. In the brain, progesterone's impact extends to serotonin receptors, potentially influencing addiction. Insufficient progesterone levels may lead to behaviors aimed at enhancing serotonin activity, such as alcohol, cannabis, and nicotine consumption. Overall, like estrogen, progesterone exhibits protective effects against skin aging and has intriguing implications in neurochemical processes.<sup>55–60</sup>

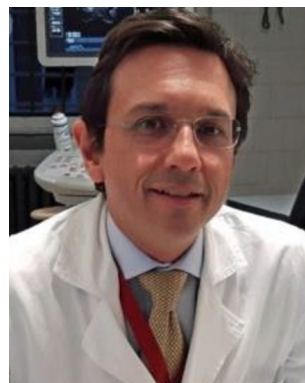
Androgens serve as the primary steroid determining sex in males; nevertheless, both males and females produce these hormones. In men, insufficient androgen levels can lead to a diminished sex drive and the development of gynecomastia.



**Andrea Lenzi**

*Professor Andrea Lenzi is Full Professor in Endocrinology at the Sapienza University of Rome. His scientific activity is characterized by over 950 publications, H. Index 94, C. Index 38864. He is President of the National Committee for Biosafety, Biotechnology and Life Sciences of the Presidency of the Council of Ministers (CNBBSV), President of the National Board of Professors in Life Sciences, President of the Sapienza School*

*of Advanced Studies (SSAS) and Chair holder of the UNESCO Chair on Urban Health.*



**Andrea Isidori**

*Professor Andrea Isidori is Full Professor in Endocrinology and Metabolic Disorder at the Sapienza University of Rome. He is also Rector's Delegate for Transdisciplinary Integration of Life Sciences at the Sapienza University of Rome. He is Director of the Molecular and Clinical Endocrinology Lab (MCEL) and is a Member of the Executive Committee of the Interdepartmental Center for Rare Diseases 'Policlinico*

*Umberto I Hospital, Rome, and of the Steering Committee of the European Neuroendocrine Association (ENEA) and the Steering Committee of the European Academy of Andrology (EAA).*



Conversely, females with excessive androgen expression may experience symptoms like hirsutism, acne, and other related issues. Testosterone, the most prevalent androgen, is produced both by the ovaries and testicles. Across all genders, androgens play crucial roles in various physiological processes, including the regulation of bone density, muscular development, onset and maturation during puberty, red blood cell production, libido, and sexual function. In men, androgens induce specific effects such as voice deepening, hair growth on the face, scalp, underarms, chest, and genitals, and the development of

sperm. In women, androgens regulate menstruation, help prevent osteoporosis by minimizing bone loss, assist in conception and pregnancy, and stimulate the growth of pubic and underarm hair.<sup>61–66</sup>

The most common techniques for the detection of sex hormones in clinical settings are direct chemiluminescent immunoassays, which do not require any pre-analysis purification, but they have demonstrated some limitations in accuracy and reproducibility.<sup>67</sup> For this reason, from 2007 the Endocrine Society has suggested the use of mass spectrometry



**Nguyen Thi Kim Thanh**

*Professor Nguyễn Thị Kim Thanh, MAE, FRSC, FInstP, FRSB, FAPS, FIMMM (<https://www.ntk-thanh.co.uk>) held a prestigious Royal Society University Research Fellowship (2005–2014). She was appointed a Full Professor in Nanomaterials in 2013 at University College London. She leads a very dynamic group conducting cutting-edge interdisciplinary and innovative research on the design and synthesis of*

*magnetic and plasmonic nanomaterials, mainly for biomedical applications. In 2019, she was honoured for her achievements in the field of nanomaterials, and was awarded the highly prestigious Royal Society Rosalind Franklin Medal. She was RSC Interdisciplinary Prize winner in 2022. She was awarded the SCI/RSC Colloids Groups 2023 Graham Prize Lectureship in recognition of an outstanding mid-career researcher in colloid and interface science. She is one of only 12 recipients globally of the 2023 Distinguished Women in Chemistry/Chemical Engineering Awards, bestowed by the International Union of Pure and Applied Chemistry (IUPAC). Currently, she is Vice Dean for Innovation and Enterprise at the Faculty of Maths and Physical Sciences. She has been Visiting Professor at various Universities in France, Japan, and Singapore. She has been invited to speak at 330 institutes and scientific meetings. She has chaired and organised over 45 high-profile international conferences. She is Editor-in-Chief of the Royal Society of Chemistry book series, Nanoscience and Nanotechnology, and an Associate Editor for Nanoscale and Nanoscale Advances journals. She edited 7 themed issues including: Theranostic nanoplatforams for biomedicine, Nanoscale, RSC (2023); Advanced Functional Nanomaterials for Biomedical Applications. Nanoscale, RSC (2021); Multifunctional nanostructures for diagnosis and therapy of diseases. Interface Focus, The Royal Society (2016); Volume 175: Physical Chemistry of Functionalised Biomedical Nanoparticles. Faraday Discussions, RSC (2014); Special issue: Functional Nanoparticles for Biomedical Applications. Nanoscale, RSC (2013); Nanoparticles Theme, Philosophical Transactions of the Royal Society A, The Royal Society (2010).*



**Riccarda Antiochia**

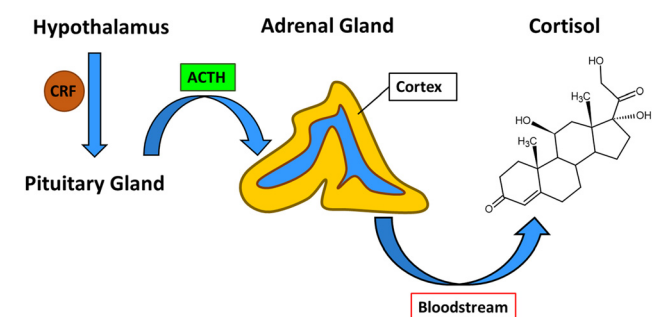
*Professor Riccarda Antiochia received an MSc degree in Chemistry with honors in 1992 and an MSc degree in Pharmacy with honors in 2009, both at the Sapienza University of Rome. In 1994 she received a Diploma of Imperial College from Imperial College, London, and in 1996 received a PhD in Chemical Sciences from the Sapienza University of Rome. In 2018 she was awarded the national scientific qualification as Full*

*Professor for the scientific sector CHIM/01, Analytical Chemistry. She is a Member of the Steering Committee of CNIS, Research Center for Biotechnology, applied to Engineering of the Sapienza University of Rome from 2011, and a Member of the PNIEC-PNRR Technical Committee of the Ministry of Environment and Energetic Security (MASE) for the environmental impact assessment of projects from Integrates National Energy and Climate Plan (PNIEC) and National Recovery and Resilience Plan (PNRR) since April 2022. She is author of 102 papers in international peer-reviewed scientific journals, 3 book chapters and 1 monograph. Her scientific activity is focused on the fields of biotechnology, nanotechnology and analytical chemistry. Her main area of research is the design and development of electrochemical (bio) sensors for clinical applications. More recently, she has been involved in the characterization of new nanostructured materials for electrode modification in second- and third-generation electrochemical biosensors, biofuel cells and microneedle-based biosensor development.*



**Table 1** Normal concentrations of cortisol, estradiol, progesterone, testosterone, insulin, TSH and GH for healthy subjects in different human body fluids

Hormone	Body fluid	Normal concentration
Cortisol	Saliva	Morning: 10.2–27.3 ng mL <sup>-1</sup> Midnight: 2.2–4.1 ng mL <sup>-1</sup>
	Hair	55 pg mL <sup>-1</sup>
	Urine	14–78 mg/day
	Serum	Morning: 250 ng mL <sup>-1</sup> Midnight: 50 ng mL <sup>-1</sup>
	Interstitial fluids	≈30 ng mL <sup>-1</sup> averaged during the day
Estradiol	Sweat	8.2–141.7 ng mL <sup>-1</sup>
	Saliva	Female: 9–15 pg mL <sup>-1</sup> Male: 2.6–10.6 pg mL <sup>-1</sup>
	Urine	Female: 30–400 pg mL <sup>-1</sup> Male: 10–50 pg mL <sup>-1</sup>
	Serum	Female: 30–400 pg mL <sup>-1</sup> Male: 10–50 pg mL <sup>-1</sup>
Progesterone	Saliva	Female: 27.1–103.6 pg mL <sup>-1</sup> Male: 15.5–49.5 pg mL <sup>-1</sup>
	Urine	Female: 0.1–0.3 ng mL <sup>-1</sup> (prepubescent), 0.1–0.7 ng mL <sup>-1</sup> (follicular stage), 2–25 ng mL <sup>-1</sup> (luteal stage) Male: 0.3–0.9 ng mL <sup>-1</sup>
	Serum	Female: 0.1–15.9 ng mL <sup>-1</sup> Male: 0.1–0.9 ng mL <sup>-1</sup>
	Testosterone	Female: 35–300 pg mL <sup>-1</sup> Male: 70–274 pg mL <sup>-1</sup>
Testosterone	Urine	Female: 2–10 mg day <sup>-1</sup> Male: 40–120 mg day <sup>-1</sup>
	Serum	Female: 15–46 ng dL <sup>-1</sup> Male: 265–923 ng dL <sup>-1</sup>
Insulin	Plasma	<1 ng mL <sup>-1</sup>
	Serum	0.2–0.4 ng mL <sup>-1</sup>
	Urine	0.1–0.8 ng mL <sup>-1</sup>
	Saliva	0.02–0.04 ng mL <sup>-1</sup>
	Tears	0.3–0.5 ng mL <sup>-1</sup>
	Milk	4.6–12.2 ng mL <sup>-1</sup>
	Interstitial fluid	1.9–3.4 ng mL <sup>-1</sup>
TSH	Cerebrospinal fluid	0.2–0.3 ng mL <sup>-1</sup>
	Serum	0.5–5.0 mU L <sup>-1</sup>
GH	Urine	0.4–4.0 mU L <sup>-1</sup>
	Serum	1.8 ± 1.2 ng mL <sup>-1</sup>
	Saliva	0.6 ± 0.5 pg mL <sup>-1</sup>
	Urine	5.1 ± 1.9 pg mL <sup>-1</sup>

**Fig. 2** Hypothalamic–pituitary–adrenal axis response chain and molecular structure of cortisol.

(MS) analysis for sex hormone characterization and quantification. Recently, in 2013, a standard assay has been developed by the National Institute of Standard and Technology (NIST)

that can analyze samples for sex hormones with liquid chromatography–mass spectrometry (LC-MS/MS).<sup>67</sup>

Testing, such as that offered by nanoparticle-based electrochemical biosensors, will greatly improve our capability to determine the concentration of and the role played by sex hormones in clinical settings.<sup>67</sup>

**1.2.3 Insulin.** Insulin is a small peptide hormone composed of 51 amino acids in total with a molecular weight of *ca.* 5.7–5.8 kDa.<sup>68,69</sup> The structure of human insulin consists of two peptide chains, namely the A-chain (21 amino acids) and the B-chain (30 amino acids), which are connected *via* two disulfide bridges. Insulin is a pancreatic hormone produced by B-cells and is responsible for regulating blood glucose levels in humans.<sup>68</sup> Our bodies respond to the presence of high blood glucose by releasing insulin, which promotes carbohydrate metabolism and glucose uptake by adipose tissue and muscle.<sup>68–70</sup> This process attempts to convert an appropriate amount of glucose into a storage form of glycogen for cellular uptake and thus reduce the circulation of glucose molecules in the bloodstream. An impairment of glucose regulation activities leads to the development of diabetes mellitus (DM), which is clinically classified into type 1 diabetes mellitus (T1DM) and type 2 diabetes mellitus (T2DM).<sup>69–72</sup> Both types of DM are characterized by an irregular increase in blood glucose, but they differ in their underlying mechanisms. T1DM is an autoimmune disease that contributes to the decline of pancreatic beta-cells and consequently hyperglycemia.<sup>72</sup> In the pathogenesis of T1DM, T-cell-mediated autoimmunity destroys beta-cells leading to a decline in beta-cell mass. As a result, patients lose the ability to produce insulin, fail to adjust blood glucose levels to normal, and eventually develop dysglycemia and symptomatic T1DM. In T1DM patients, insulin secretion is negligible or has disappeared, and treatment relies on lifetime insulin injection. Therefore, T1DM is diagnosed by the presence of T1DM-associated autoantibodies.<sup>72</sup>

On the other hand, T2DM is a significant change in blood glucose level primarily caused by insulin deficiency, insulin resistance, or both.<sup>71</sup> Insufficient insulin secretion is led by beta-cell dysfunction, resulting in the pancreas being unable to produce enough insulin to effectively control blood glucose levels. In some cases, insulin is physiologically secreted in response to rising blood glucose levels. However, the body is poorly sensitive to insulin and the glucose regulation mechanism is rarely activated, thus there is a loss of the ability to reduce blood glucose, known as insulin resistance. Since insulin resistance is a feedback regulation mechanism, insulin is continuously released in an attempt to maintain glucose at normal level. As a result, a relatively high amount of insulin is circulated in T2DM patients. In this case, elevated blood glucose levels can be detected, and patients are diagnosed with T2DM. Individuals with metabolic insulin resistance are at risk of having subsequent complications, including cardiovascular disease, blindness, high blood pressure, kidney failure, obesity, and even fatality.<sup>68,70</sup> To distinguish between these two types of DM, T2DM exhibits insulin resistance, while T1DM is characterized by the presence of autoantibodies.<sup>72</sup>



Insulin is indeed a vital biomarker, predominantly found in the bloodstream. Insulin levels can vary depending on an individual's health condition. For effective diagnosis, the association between insulin concentration and diabetes should be analysed while considering the condition of the patient. In T1DM, insulin is virtually undetectable, especially in the later stages, due to insulin deficiency. In contrast, individuals with T2DM develop insulin resistance, leading to elevated blood insulin levels.

While blood is the primary source for insulin detection, insulin hormones can also be detected in other body fluids. Excess blood insulin increases toxicity due to glucose overconsumption. In response, the body activates physiological processes to reduce blood insulin levels. The kidneys and liver play a role in regulating the level of blood insulin. The liver is primarily responsible for insulin removal and degradation, while the kidneys are involved in the reduction of insulin levels, but to a lesser extent.<sup>73</sup> In general, the kidneys diminish toxic substances and restore vital compounds to the bloodstream. In this case, blood insulin is filtered in the kidneys through the glomeruli and reabsorbed by renal tubules, a process termed insulin clearance.<sup>74</sup> In insulin clearance an appropriate amount of insulin is returned to the bloodstream and the remaining is excreted in urine.<sup>75</sup> Urinary insulin is found at low levels because most of the insulin (>98% of the glomerulus-filtered insulin) is subjected to reabsorption by proximal renal tubes.

In non-diabetic people, the insulin clearance rate is stable and independent of serum insulin. On the other hand, insulin clearance is high in T2DM, primarily due to elevated blood insulin levels, which can exceed the transport capacity of renal reabsorption. Therefore, urinary insulin can be a potential biomarker for diabetes. However, to consider urinary insulin as a biomarker, other health conditions need to be accounted for. Insulin clearance varies with creatinine clearance.<sup>74,75</sup> Furthermore, liver or kidney diseases can increase insulin clearance.<sup>74</sup> Renal disease significantly elevates urine insulin levels due to diminished tubular reabsorption of the hormone.<sup>76</sup> With derangement of kidney function, the filter mechanism is not as effective as normal, thus decreasing insulin reabsorption and increasing blood sugar level. Using urinary insulin for clinical diagnosis may be challenging with the derangement of kidney and liver functions, and careful interpretation of results is necessary.

Insulin is indeed present in blood and urine due to the insulin removal mechanism. Furthermore, it can be detected in other body fluids. A recent review has summarized the levels of insulin found in various types of body fluids.<sup>77</sup> Table 1 outlines the types of fluids and their corresponding insulin concentration ranges. As evident from Table 1, insulin is most abundant in milk and interstitial fluids. However, these fluids are not suitable for home testing, especially interstitial fluids, which require skilled medical staff and equipment for sample extraction. Among the listed fluids, serum is the preferred choice for sampling due to decent insulin content. However, other fluids such as urine and saliva hold

potential for insulin biomarkers, offering the advantages of convenience and detection, compared with traditional blood-based tests.<sup>77</sup>

Insulin in the clinical setting is mostly detected using chromatographic techniques such as high-pressure liquid chromatography (HPLC), capillary electrophoresis chromatography (EC) and, more recently, LC-MS/MS, but they require complicated procedures to prepare the samples, and costly machinery. Immunosensors have also been used to determine the concentration of insulin, but as seen for other hormones, they have a slow rate of analysis that limits their clinical use.<sup>77</sup>

**1.2.4 Thyroid-stimulating hormone.** Thyroid-stimulating hormone (TSH) is a glycoprotein hormone originating from the anterior pituitary which serves as the primary stimulus for thyroid hormone synthesis by the thyroid gland. Additionally, it induces the growth of thyroid follicular cells, leading to the enlargement of the thyroid. The release of TSH is regulated by the hypothalamic–pituitary axis. Neurons in the hypothalamus release thyroid-releasing hormone (TRH), which, in turn, stimulates thyrotrophs in the anterior pituitary to secrete TSH. TSH then prompts thyroid follicular cells to release thyroid hormones, primarily in the form of triiodothyronine (T3) or thyroxine (T4). T3, the active form of thyroid hormone, constitutes only 20% of the released hormone, with the majority of T3 originating from the peripheral conversion of T4 to T3. Thyroxine (T4), also known as tetraiodothyronine, makes up more than 80% of the secreted hormone. Upon entering circulation, T4 undergoes de-iodination to form T3. Both T4 and T3 exert negative feedback on the anterior pituitary, with elevated levels suppressing TSH secretion, and low levels stimulating TSH release. Moreover, TSH stimulates the thyroid gland to secrete prolactin.<sup>78</sup>

TSH levels are typically monitored in serum and urine samples. Table 1 presents the concentrations of TSH in these biological fluids among healthy individuals.<sup>79,80</sup>

Clinical analysis of TSH requires a great sensitivity for the different forms of the hormone. In clinical settings this is achieved by using immunoassay with sensitivity  $<0.01 \text{ mIU L}^{-1}$  or by MS/LC-MS tandem.<sup>81</sup> Electrochemical biosensors have better sensitivity, faster results and better selectivity compared with immunoassay and MS/LC-MS tandem.

**1.2.5 Growth hormone.** Growth hormone (GH) is a peptide hormone that stimulates growth, reproduction, and cell regeneration in humans. Moreover, it stimulates the production of insulin-like growth factor 1 (IGF-1) and increases the concentration of glucose and free fatty acids.

GH is secreted episodically, with approximately two-thirds of the daily secretion of GH happening during the night at the onset of slow-wave sleep, with the first episode of slow-wave sleep of the night triggering secretory pulses releasing 70% of the total daily secretion of GH. In normal healthy individuals GH has a constant minimal basal secretion over 24 h that is too low to be detected with immunoassay, which accounts for 50% of the daily amount, interrupted by peaks of secretion which account for the majority of the whole secretion. The ultradian rhythm of GH secretion is the result of the inter-



action of many different factors; for example, jet-lag temporarily increases GH peak amplitudes, physical stresses increase the levels of GH, while psychological conditions such as depression reduce GH levels.<sup>82</sup> GH secretion is also related to nutrition, with malnutrition and fasting causing an increase in GH while obesity and the ingestion of glucose suppress the secretion of GH.<sup>83</sup>

GH concentration changes in pulses, and it peaks during puberty.<sup>84</sup> In a healthy subject the concentration of GH regulates the metabolism of carbohydrates, proteins and lipids, while at the same time it stimulates the expression of insulin growth factor (IGF-1), which regulates the growth of cartilage and bones.<sup>85,86</sup>

The hyperexpression of GH is connected with gigantism or acromegaly, and the ability to detect an increase of GH peaks and concentration would give important information on the development of aggressive forms of tumours.<sup>87,88</sup>

For its action on the metabolism and the response of the body to physical exertions, GH is also considered a doping substance by the World Anti-Doping Agency.<sup>89</sup>

Concentrations of GH in biofluids other than blood have been less studied. In 2016 Gough *et al.* measured the levels of GH in serum, urine and saliva in 11 male candidates before and after physical activity (Table 1).<sup>90</sup>

Immunoassays are the most common clinical analyses for the serum concentration of GH, but recently there have been reports on the poor comparability between different immunoassays and on their analytical value.<sup>91</sup>

### 1.3 Biosensors: advantages and drawbacks compared with traditional techniques

Biosensors are appealing tools with the extraordinary capacity to detect a biological event on a transducing device utilizing a signal proportionate to the analyte concentration.<sup>92–99</sup> Both microfluidic innovations and nanotechnology advances have made easier the design and development of miniaturized devices that can operate as PoC devices.<sup>100,101</sup>

The identification of molecules in the human body specifically for the purpose of keeping track of one's health is referred to as molecular diagnostics, which covers both early and emergency diagnostics.<sup>101</sup> Early disease detection can improve patients' quality of life while they are receiving treatment and enhance the likelihood that they will survive.

Biosensors can be classified according to their recognition elements (bioreceptors) or type of transducer signal that was employed for target detection (Fig. 3A). Bioreceptors are antibodies, enzymes, DNA or aptamers, molecular imprinted polymers (MIPs), and cells. Their corresponding biosensors can be: immune-, enzymatic-,<sup>102</sup> apta-, DNA/nucleic acid (geno-), cell-based sensors (Fig. 3B).

Aptasensors are a particular class of nucleic acid biosensors, based on aptamers (single-stranded DNA/RNA) that "fit" specifically to a target. They are synthetic antibodies, DNA receptors that can replace antibodies, or complete DNA strands. MIPs are best described as synthetic analogues to the natural, biological antibody–antigen systems. As such, they

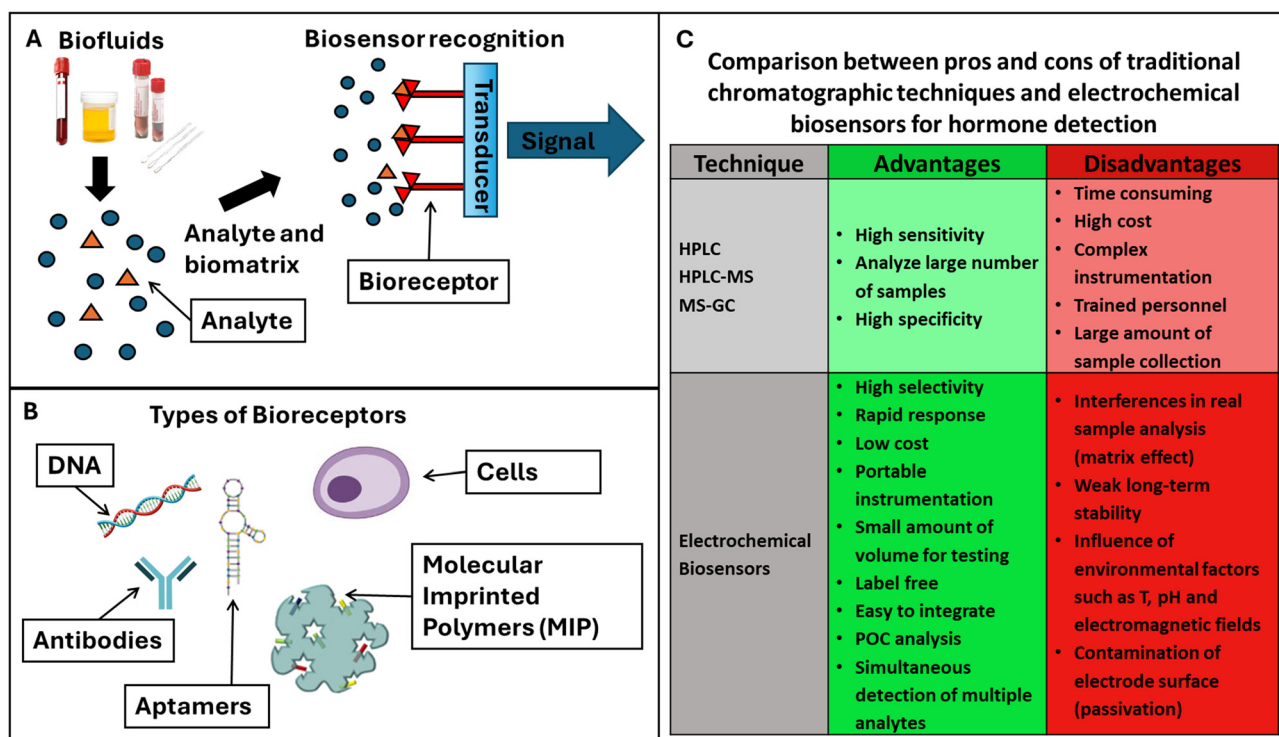


**Fig. 3** Schematic representation of (A) biosensor components, (B) types of bioreceptors and (C) comparison between the pros and cons of the traditional techniques for hormone detection and electrochemical biosensors.



operate by a “lock and key” mechanism to selectively bind the molecule with which they were templated during production. MIPs potentially offer the specificity and selectivity of the biological receptors with the explicit advantages of durability with respect to environmental conditions and low cost.

Most biosensors are based on enzymes; they can recognize the target employing electroactive species<sup>102</sup> as by-products of their enzymatic reaction. The target recognition of the bioreceptor can be quantified by measuring the transducer signal at the interface of the biosensing device.<sup>103</sup> There are several transduction signals, based on mass variations, dielectric constant, heat, and redox signal, and, consequently, biosensors can be also classified as piezoelectric, optical, calorimetric and electrochemical, respectively.<sup>104</sup> The superior characteristics of the electrochemical biosensors in terms of sensitivity and selectivity, operational simplicity and possibility of miniaturization have made these devices suitable candidates for the development of marketable PoC devices.

#### 1.4 Electrochemical biosensors

Additionally, depending on the type of transducer, the electrochemical biosensors can be subdivided into the following categories: amperometric, potentiometric, conductometric and impedimetric biosensors, depending on the interaction of the biomolecules at the electrode surface which may be generated. These sensors are based on the interaction of the biomolecules and the electrode surface, which may generate a measurable current at a particular potential (amperometric), a measurable potential or charge accumulation (potentiometric), or may alter the conductive properties of the medium (conductometric) or the charge transfer resistance (impedimetric).<sup>105</sup>

In recent years, advances in the design and synthesis of novel nanomaterials with different dimensions have enabled their incorporation into the development of biosensing electrochemical platforms, including 1D (e.g. nanotubes, nanowires, nanorods), 2D (e.g. graphene, nanosheets) and 3D (e.g. nanoparticles, quantum dots) nanomaterials. In particular, nanoparticles (NPs) have been largely used in biosensing technology electrode surface modification due to their excellent amplification of the detection signal.

Owing to their very small size (1–100 nm), they exhibit unique and very attractive chemical, physical and electronic features different from those of bulk materials, and they can be employed successfully in the development of promising electrochemical sensing devices. Usually, metal NPs present good conductivity and catalytic characteristics, which enable them to act as “electrical wires” to improve the electron transfer (ET) between the redox center of the enzymes and the electrode surface, and moreover to act as catalysts to increase the electrochemical reactions.

Many kinds of nanoparticles (metal, oxide and semiconductor ones) are widely used in electrochemical analytical devices. Their principal functions can be summarized as follows: (i) biomolecule immobilization (thanks to their large specific surface area they can strongly adsorb the bioreceptor on the electrode surface and preserve their bioactivity); (ii) catalysis of electro-

chemical reactions (due to their excellent catalytic properties); (iii) electron transfer enhancement, acting themselves as redox mediators (NPs act as mediators); (iv) labelling molecules (due to their small size and modifiability); and (v) acting as reactants (thanks to their chemical activity).<sup>106–108</sup>

For hormone detection, biosensors offer several advantages compared with the most widely used conventional techniques, such as HPLC, HPLC-M and MS-GC. Unfortunately, it is well known that these methods involve lengthy procedures and need qualified personnel to carry out the analysis. Hormone detection with electrochemical biosensors is comparatively much faster, more sensitive, and less expensive, as it does not require expensive equipment or specialists.

Moreover, biosensors allow rapid response and ease of miniaturization for PoC diagnostics.<sup>109</sup> In addition to the advantage of electronic miniaturization of electrochemical biosensors for PoC diagnostics<sup>109</sup> there are many mobile applications, and the possible integration of this technology into the internet-of-things (IoT) would help with both the real-time monitoring of patients and the rapid transmission of clinical data on infectious diseases. Moreover, the users of this diagnostic technology are able to perform an assay using their own devices, thus opening the door to easy, affordable techniques based on PoC technology. With these benefits, electrochemical biosensors are able to meet the technological needs and public health requirements of PoC, involving the widespread accessibility for people to early diagnosis and treatment of diseases.

When compared with electrochemical biosensors, the most common techniques used for the detection of hormones are expensive to perform and maintain, while requiring long sample preparations and time for analysis or lacking the necessary sensitivity to be used for clinical evaluations. Electrochemical biosensors have similar sensitivity to MS techniques without the cost and the training requirement for techniques such as MS (lengthy sample preparation) or ELISA (30 min–4 h of testing time).<sup>67</sup> The convenience and speed of electrochemical analysis allow the quick determination of multiple hormones with the same duration and resources required for a single sample.

On the other hand, biosensors have also some pitfalls such as interference in real sample analysis, weak long-term stability and contamination of the biosensor surface which, in some cases, may limit their reusability.

Fig. 3C summarizes the advantages and disadvantages of electrochemical biosensors compared with conventional chromatographic methods for hormone detection.

## 2. Nanoparticle-based electrochemical biosensors for hormone detection in biological fluids

Biofluids produced by the human body used for biosensing hormone detection are blood, urine, saliva, sweat and tears. Blood is collected from the patient with a blood draw by inserting a needle, and it is therefore an invasive procedure with



consequent patient discomfort, which may limit its application. Moreover, it has to be repeated at regular time intervals when it is necessary to measure the hormone levels over time. Serum and plasma are both fluids derived from the liquid part of the blood: serum is obtained by letting the blood clot and collecting the supernatant, while plasma is obtained by stabilizing the blood sample with anti-clotting agent (ethylenediaminetetraacetic acid, citrate *etc.*) and then separating the liquid part of the blood from the solids by centrifugation.<sup>110</sup> The use of blood, serum and plasma has been limited due to the invasiveness of the procedure to collect the samples.

Urine, saliva, sweat and tears are externally secreted biofluids which have the advantage of their non-invasive detection. In particular, urine and saliva are considered vital biofluids due to their easy accessibility and good availability. Moreover, they show good correlations with most blood analytes, which make them a valid alternative to blood analysis. The collection of urine and salivary samples is usually quick and not particularly invasive, which allows repeated sampling several times during the day.

Sweat and tears represent other interesting biofluids for their good correlation with blood, although their collection may be not always easy. For example, in many applications outside athletics, it is often necessary to use wearable bands to locally stimulate sweating.

Saliva, sweat and tears also show some limitations leading to contamination. The concentration of their bioanalytes is more variable compared with the composition of blood, and can be influenced by different factors such as the presence of microbes on the skin, in the case of sweat and tears, or by food ingestion, in the case of saliva.<sup>111</sup>

All these disadvantages may be overcome with the interstitial fluid (ISF). The ISF is definitely the most minimally invasive accessible fluid of the body. It basically acts as a mediator between blood vessels and cells in the constant supply of nutrients and removal of waste products, and therefore it represents the most reproducible matrix and shows excellent correlation with blood.<sup>112</sup> However, ISF extraction requires the realization of a complex integrated wearable device which allows extraction, collection and detection of the desired bio-

analytes in a continuous manner. Hormone detection with wearable biosensors will be discussed in section 3.

The simplest strategy for electrochemical-based monitoring of hormones is their direct electrochemical signal at the electrode surface at a specific potential. In this approach, the hormone of interest is directly oxidized or reduced at the electrode surface producing an electroactive product, which can be electrochemically measured, whose concentration is proportional to the target hormone. However, direct oxidation usually occurs at a high overpotential, which can lead to electroactive interference from other species present in the biological matrix. With regard to this, nanomaterials have been successfully utilized for electrode surface modification with the result of higher selectivity. However, to better address this issue, indirect detection methods have been realized based on the use of specific biorecognition elements coupled to the electrode surface, allowing for sensitive and selective detection of the target hormone.

The electrochemical nanoparticle-based biosensors described in this review, namely immunosensors, aptasensors, and MIP-based biosensors, depending on which biorecognition element is used, *i.e.* antibodies, aptamers, or MIPs, respectively, may involve direct, competitive, or sandwich configurations and label-free or label-based approaches. Less frequently enzymes are employed, corresponding to the so-called enzymatic biosensors.

In the following, various recent electrochemical detection strategies used for measuring selected hormones in several sample matrices are presented, and are schematized in Fig. 4.

## 2.1 Detection of cortisol

Cortisol is not an electroactive molecule and lacks a specific enzyme catalysing its redox reaction. Consequently, most cortisol biosensors are affinity biosensors based on bioreceptors, such as antibodies (immunosensors), aptamers (aptasensors) and MIPs.

Regular sampling and analysis of cortisol concentrations during the day is fundamental for studying the metabolic behaviour of a hormone that naturally has a peak of concen-

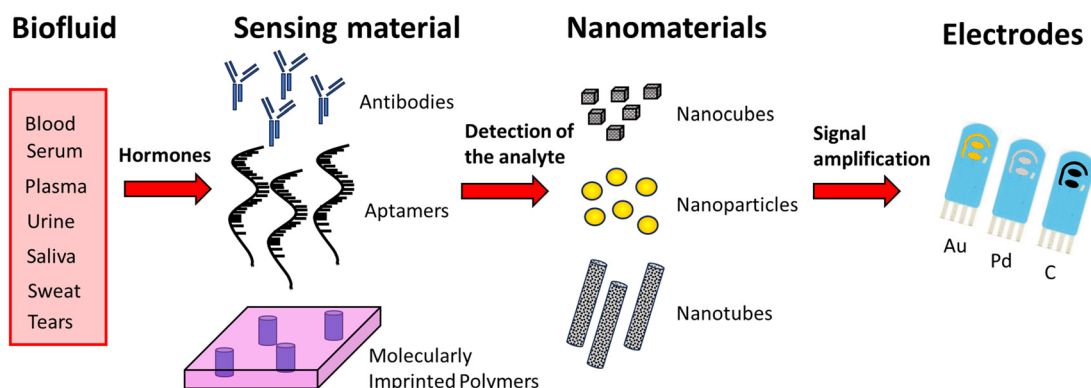


Fig. 4 General principle of nanoparticle-based electrochemical biosensors for detecting hormones from biological fluids.



**Table 2** Electrochemical nanoparticle-based biosensors for cortisol detection

Nanoparticles	Electrode	Receptor	Transducer	Bodily fluid	LOD	Linear range	Ref.
AuNPs	Au	Aptamers	DPV	Saliva	0.8 pM	0.28 pM–0.28 μM	114
Ni nanoclusters-N-CNT	GCE	MIP	DPV	Saliva	2.37 fM	10 fM–1 nM	115
AuNPs/MoS <sub>2</sub> /AuNPs	C	AntiC	DPV	Saliva	0.18 nM	0.5 nM–200 nM	116
SmMoO <sub>4</sub> nanoflowers	GCE	Aptamers	DPV	Saliva	45 fM	100 fM–10 pM	113
AuNPs	Au	MIP	SWV	Saliva	200 fM	1 pM–0.5 μM	119
NiCo-MOF/SnS <sub>5</sub> -Thioacetamide/AuNPs	GCE	AntiC	SWV	Saliva	80 fM	0.28 pM–0.28 μM	120
CuWO <sub>4</sub> @MoS <sub>2</sub> NPs/Chitosan-AuNPs	GCE	AntiC	CV	Saliva	38.6 aM	2.8 fM–2.8 μM	122
ZnO nanoflakes	Au	AntiC	CV	Saliva	1 pM	100 pM–100 nM	123
ZnO nanorods	Au	AntiC	CV	Saliva	1 pM	10 pM–100 nM	123
DNA–AuNPs superlattice	Au	Aptamers	EIS	Saliva	0.13 nM	0.5 nM - 10 nM	124
MWCNTs/AuNPs	PDMS	AntiC	DPV	Sweat	0.83 fM	2.8 fM–2.8 μM	125
AgNPs and AuNPs	GCE	Aptamers	DPV	Sweat	0.25 pM	0.28 pM–28.6 nM	126
Fe <sub>2</sub> O <sub>3</sub> nanosized ellipsoid	Carbon Yarn	AntiC	CV	Sweat	8.3 aM	2.8 fM–2.8 μM	127
MnO <sub>2</sub> nanocacti	GCE	AntiC	EIS	Sweat	23 fM	0.1 pM–1.5 nM	128
ZnO nanocrystals	Pd	AntiC	EIS	Sweat	2.8 nM	27.6 nM–0.5 μM	129
Ag@AgO core/shell	Au	AntiC	CV	Serum	1.8 pM	2.8 pM–2.8 μM	130
Fe <sub>3</sub> O <sub>4</sub> NPs and AuNPs	GCE	AntiC	DPV	Serum	0.14 nM	0.28 nM–2.8 μM	131
AuNPs	Au	AntiC	SWV	Blood	44.1 pM	137.9 pM–6.9 nM	132

tration in the morning and slowly decreases with time to reach a minimum around midnight.

Table 2 summarizes the characteristics and performances of nanoparticle-based electrochemical biosensors for cortisol in the literature.

**2.1.1 Saliva samples.** Cortisol concentrations in saliva are always fairly low, less than  $\approx 30$  ng mL<sup>-1</sup> in the morning and as low as 2.2 ng mL<sup>-1</sup> at night, which requires the development of very sensitive sensors.<sup>113</sup>

**2.1.1.1. Voltammetric biosensors.** Examples of DPV electrochemical biosensors for the detection of cortisol in saliva can be found in the work of Sharma V. *et al.*, Duan D. *et al.*, Liu J. *et al.* and Rezapoor-Fashtali Z. *et al.*<sup>113–116</sup>

Sharma V. *et al.* in 2023 developed an electrochemical sensor based on a printed Au electrode on which AuNPs are deposited and then functionalized with aptamers to detect cortisol.<sup>114</sup>

Liu J. *et al.* (Fig. 5A) described an electrode based on a AuNP-modified carbon electrode, on which a layer of MoS<sub>2</sub> was deposited. On it another layer of AuNPs was deposited and modified with a PEG-COOH attached to antibodies. In this work the AuNPs were used both to anchor the different layers of the sensor and to improve the electrical contact between the electrode and the antibody. One of the advantages of this sensor was that it was easily controlled using a smartphone app.<sup>116</sup>

Duan D. *et al.* in 2022 (Fig. 5B) offered a different approach for the construction of a biosensor; their DPV electrochemical sensor was based on a glass carbon electrode on which were dropped nitrogen-doped carbon nanotubes modified with nickel nanoclusters (NiNCs-N-NCTs). The presence of the NiNCs-N-NCTs on the surface of the electrode greatly expanded the surface area and the sensitivity of the sensor, thus allowing it to register the minute change in current caused by the binding of cortisol on the matrix formed by the polymerization of *o*-phenylenediamine in the presence of cortisol (0.5 mM). After reticulation the polymer formed was able to retain cav-

ities in the shape of the molecules of cortisol present during the process, creating sites where cortisol in the sample could interact. According to Duan D. *et al.* the bamboo-like structure of the electrode improved the transmission of the signal from the MIP to the electrode, thus providing an enhancement of the signal detected.<sup>115</sup>

Rezapoor-Fashtali Z. *et al.* (Fig. 5C) for their sensor utilized samarium molybdate (SmMoO<sub>4</sub>) nanoflowers deposited on a glassy carbon electrode (GCE) and trapped in a layer of polypyrrole (PP). The resulting mesh was then covered with reduced graphene oxide (r-GO). On this base, aptamers were attached by exploiting their terminal -NH moiety and used to interact with cortisol. In this set up the layer of r-GO maintained a weak negative charge that slightly repelled DNA sequences (negatively charged), thus preventing entanglement and improving the interaction with cortisol. The sensor required 15 min of incubation in a solution containing the analyte in order to maximize its response to the presence of cortisol.<sup>113</sup>

Another interesting voltammetric technique is SWV, which is faster than DPV and can sometimes offer better sensitivity and be less affected by non-faradaic currents, although it is less suitable for very diluted samples.<sup>117,118</sup>

Both Yeasmin S. *et al.* and Yang B. *et al.* applied SWV to the detection of cortisol in salivary fluid, while utilizing different electrodes and methods of detection.<sup>119,120</sup> In the work of Yeasmin S. *et al.*, AuNPs and a MIP were formed on the surface of a gold-plated electrode. The reactions which led to the simultaneous formation of Au NPs and MIP were done by applying between 0 V to 1 V to a solution of *o*-phenylenediamine and H<sub>2</sub>AuCl<sub>4</sub> in the presence of cortisol. The resulting polymer had Au NPs trapped in its matrix and, after washing, cavities shaped like molecules of cortisol. During the analysis of a sample some of the cavities were occupied by cortisol, and the amount of current passing through the electrode was reduced.<sup>119</sup>

Yang B. *et al.* used a complex metal-organic framework (MOF) electrode based on a combination of Ni(NO<sub>3</sub>)<sub>2</sub>, K<sub>3</sub>[Co



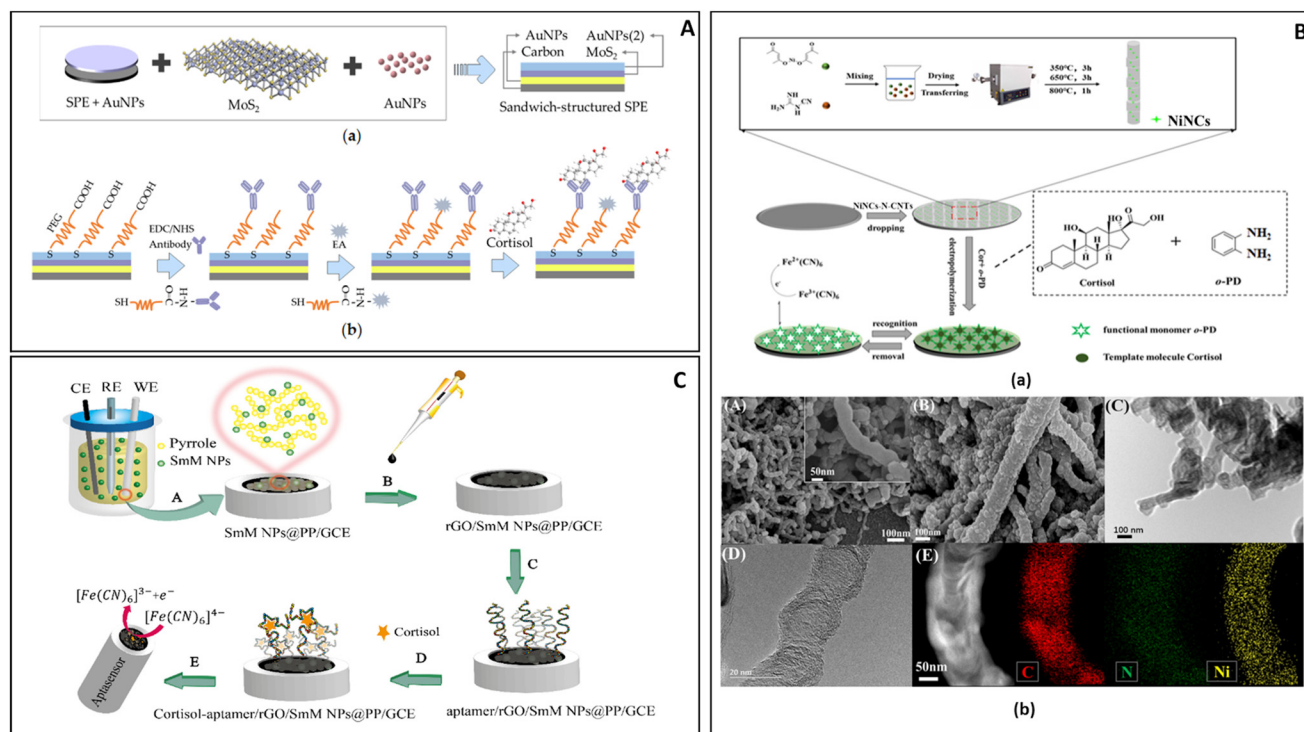


**Fig. 5** (A) The construction and detection procedure of cortisol immunosensor: (a) fabrication of layer-by-layer self-assembled gold nanoparticles/molybdenum disulfide/gold nanoparticles (AuNPs/MoS<sub>2</sub>/AuNPs) sandwich-structured screen-printed electrode (SPE), (b) covalent immobilization of cortisol antibody through self-assembled monolayer of polyethylene glycol (PEG).<sup>116</sup> (B) Preparation of the NiNCs/MIP electrode and SEM characterization: (a) multisteps fabrication of the NiNCs-N-CNTs/GCE electrode and MIP layer, (b) SEM images of NiNCs-N-CNTs (A) and MIP/NiNCs-N-CNTs (B), TEM images of MIP/NiNCs-N-CNTs (C) and NiNCs-N-CNTs (D), STEM-EDS mapping (C, N and Ni elements) of NiNCs-N-CNTs (E).<sup>115</sup> (C) APTASensor design: (A) electro-polymerization to form polymeric nanocomposites, (B) rGO dropping, (C) aptamer loading, (D) aptasensor immersion in the cortisol solution, (E) electro-chemical investigation of ferricyanide as a probe on the surface of the aptasensor.<sup>113</sup>

(CN)<sub>6</sub> and SnS<sub>2</sub>. The NiCo-MOF was shaped as nanocubes and embedded in a matrix of SnS<sub>2</sub> and thioacetamide. In the same matrix AuNPs were formed. On this complex structure monoclonal antibodies were attached and used to detect cortisol.<sup>120</sup>

CV is a fundamental technique for the study of redox reactions, based on the fast application of a potential range to a sample while measuring the current produced.<sup>121</sup>

Nong C. *et al.* developed an electrochemical biosensor for cortisol in saliva based on a modified glassy carbon electrode (GCE) on which core shell particles of CuWO<sub>4</sub> covered in MoS<sub>2</sub> were deposited. On the functionalized surface of the electrode a network of chitosan decorated with AuNPs was layered and functionalized with anti-cortisol monoclonal antibodies; foetal bovine serum (FBS) was then used to reduce the possibility of non-specific binding.<sup>122</sup>

Vabbina P.K. *et al.* have developed two electrochemical biosensors based on ZnO nanoflakes or ZnO nanorods immobilized on a gold electrode (Fig. 6A). On these nanostructures antibodies were attached and used to detect the presence of cortisol.<sup>123</sup>

The width of the linear range for this system does not completely represent the differences between the two particles' morphology tested by Vabbina *et al.*; ZnO nanorods were able to give a linear response for quantities of cortisol 10 times

smaller than the flakes, but the larger exposed surface of the flakes and their shape improved the contact with the electrode and the binding with the antibody, thus generating sharp and defined peaks when used for CV. This gain in resolution and the relative ease of manufacture made the ZnO nanoflakes the most likely candidate for further development.

**2.1.1.2. Impedimetric biosensors.** Cantelli *et al.* used EIS for cortisol detection, a technique able to collect information about the processes happening on the electrode surface by measuring the fluctuations of impedance caused by the biorecognition process at the electrode surface in the presence of a redox probe in solution (Fig. 6B). In this work the authors have realized a superlattice of DNA sequences attached to an Au electrode and attached to AuNPs and to specific aptamers.<sup>124</sup>

**2.1.2 Sweat samples.** According to the most cited studies, sweat can contain between 8.16 ng mL<sup>-1</sup> and 141.7 ng mL<sup>-1</sup> of cortisol, a concentration comparable to blood and plasma.<sup>34</sup> Recently, there has been new evidence that these values may have been overestimated, with the actual concentration of cortisol in sweat attested to be around 0.5 ng mL<sup>-1</sup> (1.4 nM) to 1.7 ng mL<sup>-1</sup> (4.7 nM), with large variations caused by the stress level and the diet.<sup>111</sup>

**2.1.2.1 Voltammetric biosensors.** DPV is one of the most commonly used techniques for analysing the concentration of



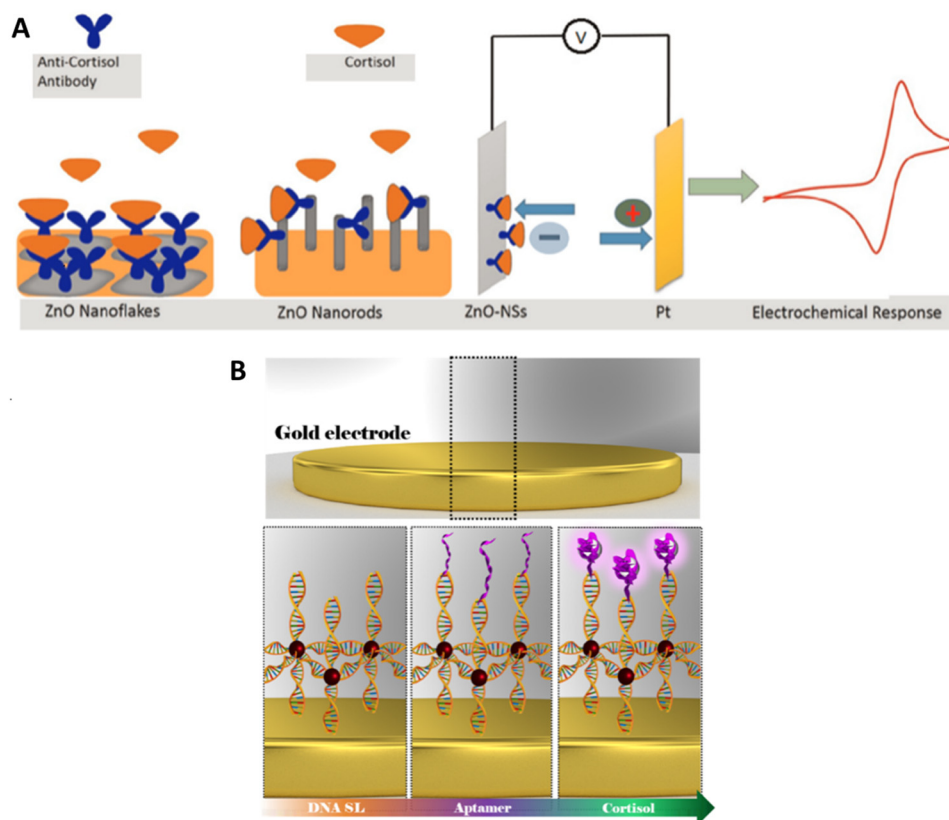


**Fig. 6** (A) Illustration of ZnO-nanorods and ZnO-nanoflakes immobilized on gold electrodes and functionalized with monoclonal anti-cortisol antibody (left); electrochemical response at the fabricated electrodes (right).<sup>125</sup> (B) Structure of the superlattice/AuNPs/Aptamer biosensor.<sup>124</sup>

cortisol in sweat samples. Obviously, several different electrochemical platforms and different NPs have been employed for electrode modification. Liu *et al.* used multi-walled carbon nanotubes (MWCNTs)<sup>125</sup> to increase the sensitivity of thin microelectrodes, whereas Huang *et al.* in 2021 used MWCNTs in combination with mesoporous carbon material (CMK-3) bound with chitosan and decorated with Ag NPs as a way to detect the presence of cortisol in sweat.

The voltammetric biosensor described by Liu *et al.* was formed by a thin layer of MWCNTs supported on a film of polydimethylsiloxane (PDMS), which was functionalized with AuNPs and cortisol-specific antibody (Fig. 7A). Later the electrode was incubated with BSA to saturate all the locations for nonspecific binding. The prepared electrochemical biosensor was thin and flexible enough to be worn as a patch and detect the level of cortisol in real-time.<sup>125</sup>

Z. Huang *et al.* described an electrochemical biosystem based on a GCE electrode on which MWCNTs and CMK-3 were deposited and blocked with chitosan (Fig. 7B). On this decorated surface, Ag NPs were adsorbed and used as support for aptamers, which were able to bind cortisol with antibodies and Au NPs which were used to produce the analytical signal.<sup>126</sup>

CV is relatively less popular as a detection technique for cortisol in sweat samples; however, Sekar *et al.* have success-

fully created an electrochemical biosensor based on this technique.<sup>127</sup> The proposed biosensor was fabricated by deposition of nanosized ellipsoidal  $\text{Fe}_2\text{O}_3$ , 300–350 nm in diameter and 850 nm in length, on a carbon yarn, followed by the immobilization of cortisol-specific antibodies. The excess of non-specific binding sites was blocked by BSA. The proposed immunosensor was able to fully analyse sweat samples in only 120 s.<sup>127</sup>

**2.1.2.2. Impedimetric biosensors.** Zhou *et al.* developed a biosensor based on  $\text{MnO}_2$  nanostructures, while Munje *et al.* developed a biosensor based on the deposition of NPs of ZnO on the surface of polyamide substrate.<sup>128,129</sup>

Zhou *et al.* studied the possibility of fabricating an electrochemical biosensor based on  $\text{MnO}_2$  nanostructures as nanorods,  $\text{MnO}_2$  nanoparticles/carbon and  $\text{MnO}_2$  nanocacti (Fig. 8A). Nanocacti are nanoparticles of approximately spherical structure with spikes and crumpled thin surfaces similar to the leaves of a succulent plant. Of the three nanostructures only  $\text{MnO}_2$  nanocacti showed some resistivity, which is necessary for EIS analysis. These structures were used to form the biosensors, modified with monoclonal antibodies for cortisol, and the non-specific binding sites blocked with BSA.<sup>128</sup>

The last NP-based electrochemical biosensor for the detection of the concentration of cortisol in sweat based on EIS listed in this review was developed by Munje *et al.* (Fig. 8B). In



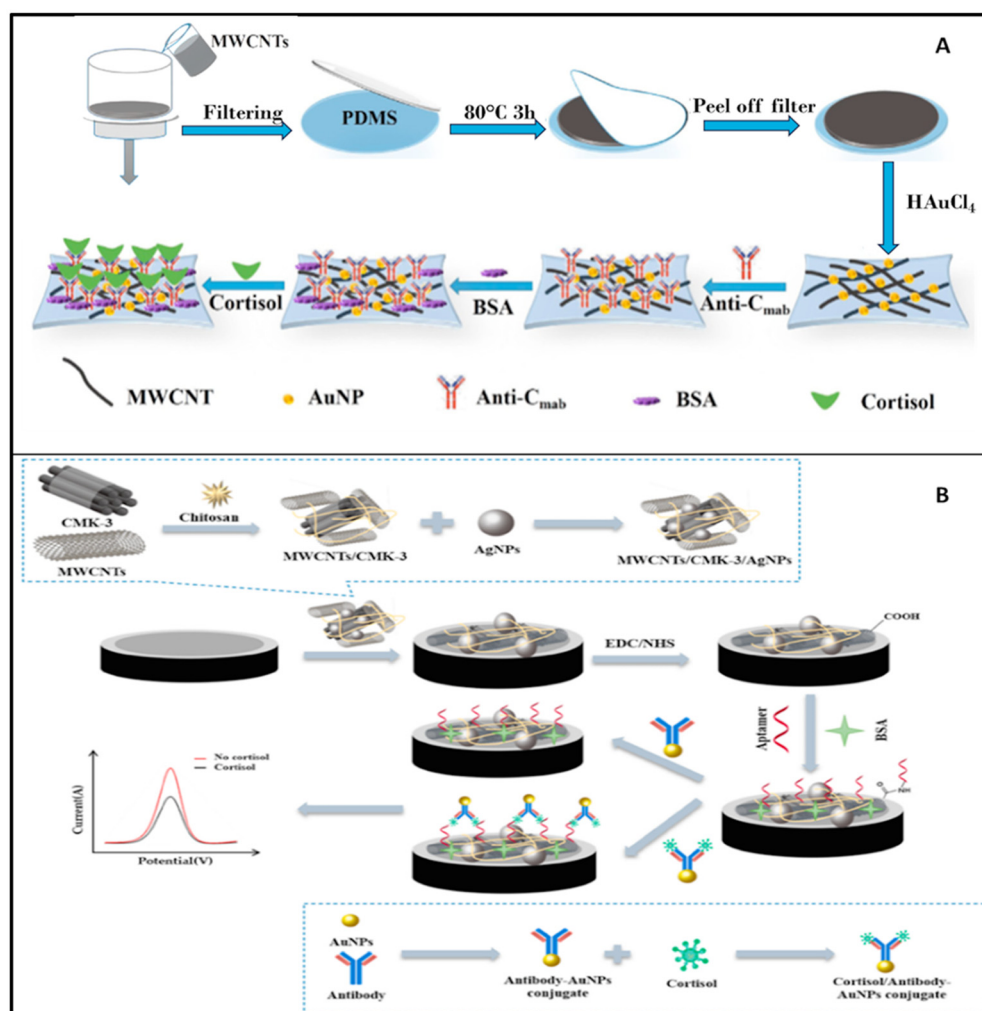


Fig. 7 (A) Stepwise fabrication of the immunosensor (Anti-C<sub>mab</sub>/AuNPs/MWCNTs/PDMS);<sup>125</sup> (B) preparation and functioning of the cortisol sensor described by Huang *et al.*<sup>126</sup>

their work, Munje *et al.* deposited a thin layer ( $\approx 90$ – $100$  nm) of ZnO on a polyamide matrix by pulsed laser deposition; on this layer antibodies specific for cortisol were attached by using dithiobis(succinimidyl propionate) (DSP) as crosslinker.<sup>129</sup>

This system was on the threshold between nanostructured material and true NPs; the pores in the polyamide matrix were nanosized, as were the ZnO nanocrystals laser deposited on it, but in its complex the structure was macroscopic.

**2.1.3 Other body fluids.** Although the initial stage of cortisol biosensing used only blood serum as a sample, only a few papers have been reported in the literature in recent years for the detection of cortisol in blood and serum, which have been now overtaken by sweat and saliva for their non-invasive nature of detection.

Both Kaushik *et al.* and Sun *et al.* developed two immunosensors to detect cortisol in human serum.<sup>130,131</sup> Kaushik *et al.* developed an electrochemical biosensor based on alternate electrodeposition of layers of polyalanine and core-shell Ag@AgO NPs on a gold electrode. On the modified electrode,

monoclonal antibody for cortisol was attached and non-specific adsorption was prevented by the deposition of BSA on the surface of the electrode. The presence of cortisol and its concentration was established by CV.<sup>130</sup>

Sun and collaborators developed an electrochemical biosensor based on a glass carbon electrode (GCE) covered in Nafion on which a layer of polyethylenimine graphene oxide (rGO-PEI) modified with Fe<sub>3</sub>O<sub>4</sub> NPs was attached. On the electrode a layer of AuNPs was also deposited. Cortisol was attached to the surface of the electrode and used as an anchor point for monoclonal cortisol antibodies modified with an enzyme able to induce the dimerization of phenylethylenediamine in the presence of H<sub>2</sub>O<sub>2</sub> which could be detected by DPV.<sup>131</sup>

Liu *et al.* have developed an electrochemical biosensor for detecting the presence of cortisol in blood samples. On an Au electrode, AuNPs were deposited; on this substrate thiolated protein G and monoclonal antibodies for cortisol were attached and tested using SWV.<sup>132</sup>



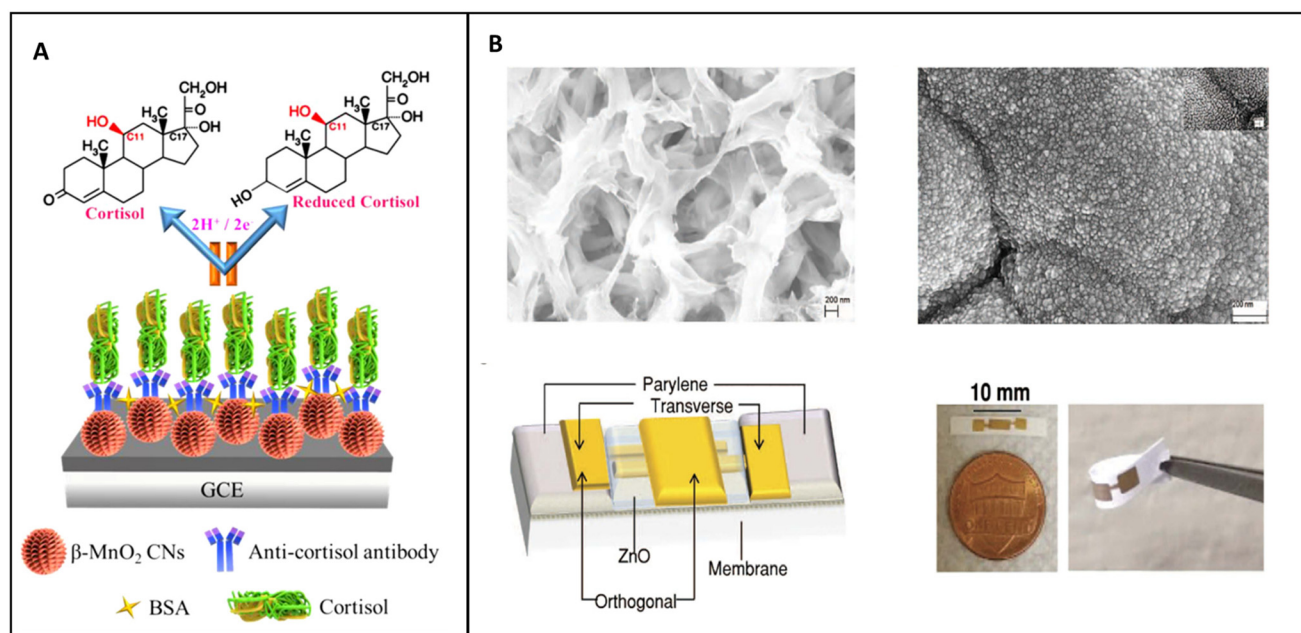


**Fig. 8** (A) Schematic representation of  $\text{MnO}_2$  nanocacti electrochemical biosensor;<sup>128</sup> (B) TEM pictures of the polyamide matrix before and after the deposition of ZnO, scheme of the electrochemical biosensor and real-life image of the biosensor.<sup>129</sup>

## 2.2 Sex hormones

Most electrochemical biosensors for the three main sex hormones, estradiol, testosterone and progesterone, in all biological samples reported in the literature are based on antibodies and enzymes. Table 3 summarizes the characteristics and performances of NP-based electrochemical biosensors for estradiol, progesterone and testosterone in the literature.

**2.2.1 Urine samples.** Analyzing urine for the detection of sex hormones has been a potential avenue, yet its application has been constrained by the nature of the sample collection procedures.

**2.2.1.1 Voltammetric biosensors.** CV was often used for the detection of the three sex hormones. Sanli *et al.* developed a portable testosterone biosensor based on the use of a screen-

printed working electrode (SPWE) functionalized with magnetic NPs (MNPs), in particular iron oxide NPs.<sup>133</sup> The designed biosensor was tested by CV using a spiked synthetic urine sample, and demonstrated a high selectivity and sensitivity towards testosterone, with a linear range between 50 and 1000  $\text{ng mL}^{-1}$  and LOD value of 23.68  $\text{ng mL}^{-1}$ .<sup>133</sup>

DPV was also often used because of its superior sensitivity. Huang *et al.* used AuNPs for the design of a selective and sensitive enzyme biosensor for 17- $\beta$ -estradiol.<sup>134</sup> A GCE was modified with copper sulfide nanosheets (CuS) that acted as electrical conductor, and the dual modification of glucose oxidase and gold nanoparticles (AuNPs) on the electrode generated the electrochemical signal amplification. The combination of AuNPs and CuS nanosheets favored the electron transfer and amplified the DPV electrochemical

**Table 3** Electrochemical nanoparticles-based biosensors for sex hormones detection

Sex hormone	Nanoparticle	Electrode	Receptor	Transducer	Bodily fluid	LOD	Linear range	Ref.
Testosterone	MNPs	SPE	Antibody	CV	Urine	23.7 $\text{ng mL}^{-1}$	50–1000 $\text{ng mL}^{-1}$	133
Estradiol	AuNPs	GCE	Enzyme	DPV	Urine	$6.0 \times 10^{-14}$ M	$5.0 \times 10^{-13}$ – $5.0 \times 10^{-9}$ M	134
Estradiol	RhNPs	GCE	Enzyme	DPV	Urine	0.54 pM	0.9–11 pM	135
Estradiol	AuNPs	GCE	Aptamer	DPV	Urine	0.7 pM	0.001–1 nM	136
Estradiol	AgNPs	GCE	Antibody	Amperometry	Urine	65 $\text{pg mL}^{-1}$	0.1–50 $\text{ng mL}^{-1}$	137
Progesterone	N-HCSs	GCE	Aptamer	DPV	Urine	$3.3 \times 10^{-6}$ nM	$1 \times 10^{-5}$ – $4.2 \times 10^{-3}$ nM	138
Estradiol	AuNPs	GCE	Aptamer	DPV	Serum	1.5 pM	12 pM–60 nM	140
Estradiol	AuNPs	SPCE	Antibody	CV, DPV	Serum	10 $\text{pg mL}^{-1}$	0.01–100 $\text{ng mL}^{-1}$	141
Estradiol	AuNPs	Au electrode	Antibody	SWV	Serum	0.84 $\text{pg mL}^{-1}$	$0.54$ – $1.36 \times 10^4$ $\text{pg mL}^{-1}$	142
Estradiol	AuNPs	GCE	Aptamer	DPV	Serum	5 $\text{pg mL}^{-1}$	0.01–500 $\text{ng mL}^{-1}$	143
Estradiol	Au@Pt	GCE	Aptamer	DPV	Serum	$8.0 \times 10^{-14}$ M	$1.0 \times 10^{-13}$ – $1.0 \times 10^{-9}$ M	144
Progesterone	NiO-AuNFs	SPCE	Aptamer	DPV	Serum	0.58 $\text{pg mL}^{-1}$	0.003–314.46 $\text{ng mL}^{-1}$	145
Progesterone	AuNPs	GCE	MIP	SWV	Serum	0.17 nM	0.2–125 nM	146
Testosterone	AuNPs	ITO glass	Antibody	EIS	Saliva	3.9 $\text{ng mL}^{-1}$	10 $\text{ng mL}^{-1}$ –0.5 $\mu\text{g mL}^{-1}$	149



signal; this made it possible to obtain a high sensitivity with a LOD of 60 fM.<sup>134</sup>

Povedano and colleagues developed an electrochemical enzymatic biosensor based on rhodium nanoparticles (RhNPs) for 17- $\beta$ -estradiol detection.<sup>135</sup> The innovative platform was obtained by a one-pot reaction that generated a nanomaterial based on graphene oxide/Rhodium nanoparticles (rGO/RhNPs). In particular, the simultaneous reduction of Rhodium (III) chloride (RhCl<sub>3</sub>) and graphene oxide with sodium borohydride (NaBH<sub>4</sub>) generated a novel platform subsequently drop-casted onto a GCE. The rGO/RhNPs/GCE was used as a support for binding the laccase enzyme, thus obtaining a biosensor used for 17- $\beta$ -estradiol monitoring. The DPV showed a high sensitivity, high selectivity and a low LOD (0.54 pM) for the designed biosensor.<sup>135</sup>

Huang *et al.* developed a sensitive aptasensor based on a thiol group-tagged 17- $\beta$ -estradiol aptamer on a GCE previously modified with AuNPs and cobalt sulfide nanosheets (CoS) for monitoring the level of 17- $\beta$ -estradiol in a urine sample.<sup>136</sup> Through differential pulse voltammetry it was possible to evaluate the LOD value and the linear concentration range, 0.7 pM and 0.001–1 nM, respectively. This electrochemical aptamer biosensor based on a hybrid nanomaterial composed of AuNPs and CoS demonstrated high sensitivity, high selectivity and good stability.<sup>136</sup>

AgNPs were used by Cincotto *et al.* to build an immunosensor for estradiol monitoring.<sup>137</sup> After the synthesis of mesoporous silica-coated reduced graphene oxide (SiO<sub>2</sub>/GO), that allowed the anchoring of metal NPs safely onto the graphene support and favouring the catalytic performance, AgNPs were used to obtain the AgNPs/SiO<sub>2</sub>/GO hybrid. This hybrid structure was adsorbed onto the GCE and then grafted with 4-aminobenzoic acid to create a desirable surface for covalent bonding of the capture antibody. This strategy allowed the development of a competitive immunosensor for the determination of estradiol hormone that exhibited good reproducibility and stability, a linear range between 0.1 and 50 ng mL<sup>-1</sup> and a LOD of 65 pg mL<sup>-1</sup>.<sup>137</sup>

Ghanbarzadeh *et al.* have developed a novel non-invasive sensor aimed at monitoring progesterone levels.<sup>138</sup> In their study, they designed an ultrasensitive electrochemical aptasensor capable of detecting progesterone in human urine. The sensor utilized nitrogen-doped hollow carbon spheres (N-HCSs) to covalently immobilize high-density aptamer (Apt) sequences, which served as the bioreceptor for progesterone. To fabricate the sensor, N-HCSs were dropcast onto the surface of a GCE, followed by the addition of Apt specific to progesterone onto the N-HCS-modified electrode. Subsequently, BSA was employed as a blocking agent to prevent nonspecific interactions. By employing DPV, the sensor demonstrated a limit of detection (LOD) value of 3.33 fM and a linear concentration range spanning 10 fM to 5.6  $\mu$ M. This aptasensor exhibited a high selectivity even in the presence of various off-target species, showcasing its effectiveness in detecting progesterone in human urine samples.<sup>138</sup>

**2.2.2 Serum samples.** The biosensors used for sex hormone detection in serum samples were obtained by the

modification of SPWE, GCE or other types of electrode with different types of NPs to obtain sensitive and selective platforms.

**2.2.2.1 Voltammetric biosensors.** Electroanalytical techniques such as linear sweep voltammetry (LSV), CV, DPV, SWV, and chronoamperometry offer comprehensive qualitative and quantitative insights into electroactive species. Consequently, they are increasingly recognized as potential alternatives to more traditional spectrometric or chromatographic techniques. These methods are extensively employed for monitoring various hormones, including sex hormones, owing to their ability to provide detailed information on their concentrations and behavior.<sup>139</sup>

A novel nanocomposite based on the interaction between AuNPs and thionine (Thi) was studied by Liu and colleagues to develop an electrochemical aptasensor to quantify the concentration of 17- $\beta$ -estradiol in serum samples.<sup>140</sup> The cationic dye Thi was used as electrochemical indicator and was mixed with carbon nanotubes (CNTs) to form a Thi/CNTs composite. After that, the Thi/CNTs solution was added into an AuNP solution, forming AuNP/Thi/CNTs, and this support was cast onto a GCE. The designed platform modified with a specific aptasensor was studied by DPV in the presence of different concentrations of 17 $\beta$ -estradiol, and exhibited a very low limit of detection of 1.5 pM and a linear range from 12 pM to 60 nM.<sup>140</sup>

In another work AuNPs were combined with carbon nanotubes (CNTs) to obtain an electrochemical immunosensor for 17- $\beta$ -estradiol detection.<sup>141</sup> Wang *et al.* fabricated a microfluidic device based on AuNPs, MWCNTs and Thi used to modify a SPWE. In this designed composite, Thi molecules acted as electrochemical mediator while MWCNTs and AuNPs, like any nanomaterials, favouring electron transfer for the signal amplification. The synergistic effect of electrochemical mediator and catalytic material produced a sensitive electrochemical immunosensor that revealed a low limit of detection of 10 pg mL<sup>-1</sup>.<sup>141</sup>

SWV was also utilized. Moneris *et al.* designed a sensitive immunosensor based on AuNPs for 17- $\beta$ -estradiol (17 $\beta$ -E) monitoring in real bovine serum samples.<sup>142</sup> The immunosensor was constructed on a gold disk electrode modified with a simple layer of cysteamine (Cys-Au electrode) grafted with AuNPs. Over this structure was immobilized the anti-17 $\beta$ -E monoclonal antibody (mAbE), thus obtaining a highly sensitive and selective immunosensor towards the target molecule (Fig. 9).<sup>142</sup>

Ming *et al.* have introduced a novel folding aptasensor platform featuring microfluidic channels specifically designed for the label-free electrochemical detection of 17- $\beta$ -Estradiol.<sup>143</sup> They utilized an innovative nano-assembly comprising amine-functionalized SWCNTs, methylene blue, and AuNPs to modify a GCE working electrode, thereby enhancing the detection sensitivity for estradiol. The calibration curve derived from experimental data demonstrated a linear range spanning from 10 pg mL<sup>-1</sup> to 500 ng mL<sup>-1</sup>, with an achieved detection limit of 5 pg mL<sup>-1</sup>. Moreover, the platform underwent experiments for E2 detection in clinical serum, yielding results highly comparable



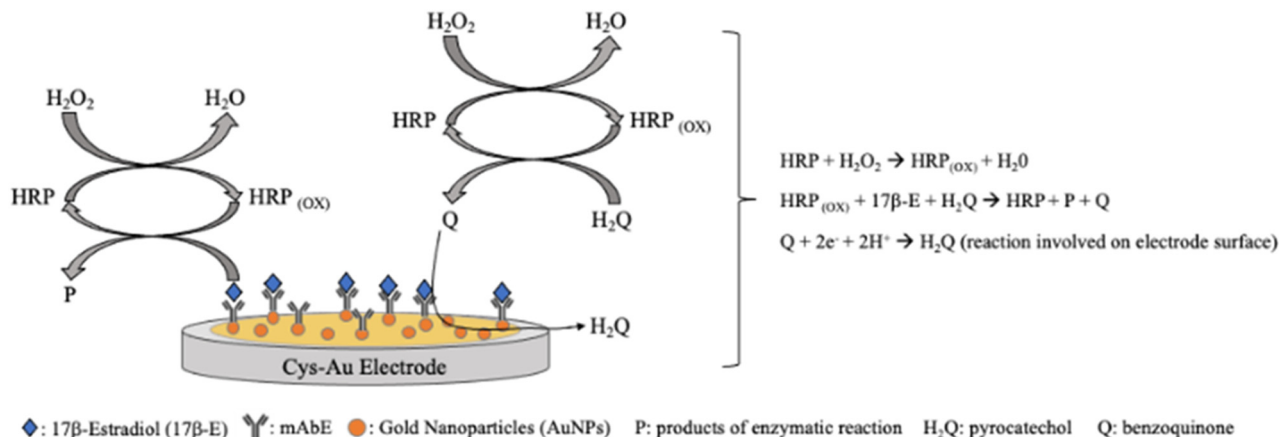


Fig. 9 Schematic presentation of the 17-β-estradiol electrochemical immunosensor based on Cys-Au electrode modified with gold nanoparticles and anti-17-β-estradiol monoclonal antibody.<sup>142</sup>

to those obtained using large electrochemical luminescence apparatus. The proposed device is a portable, inexpensive, and highly sensitive aptasensor platform that is capable of detecting estradiol with high resolution in a real human sample.<sup>143</sup>

Zhao *et al.* have presented another electrochemical aptasensor tailored for monitoring 17-β-estradiol in serum samples.<sup>144</sup> They electrodeposited poly(3,4-ethylenedioxythiophene) (PEDOT)-graphene oxide (GO) coupled with Au@Pt nanocrystals (Au@Pt) onto a GCE. Notably, the Au@Pt nanocrystals, synthesized through a one-step reaction, were utilized for immobilizing the aptamer specific to 17-β-estradiol, thereby enhancing detection sensitivity. Upon the addition of 17-β-estradiol the signal obtained through DPV gradually decreased. Under optimal conditions, the calibration curve for 17-β-estradiol displayed a linear range spanning from 0.1 pM to 1 nM, with an impressively low LOD of 0.08 pM. The developed aptasensor exhibited high selectivity, stability, and reproducibility.<sup>144</sup>

An electrochemical progesterone aptasensor was successfully developed by Samie *et al.*<sup>145</sup> They utilized NiO-Au hybrid nanofibers (NiO-AuNF) synthesized *via* the electrospinning technique, combined with graphene quantum dots (GQDs) along with MWCNTs to modify a screen-printed carbon electrode (SPCE). This modification aimed to create an effective immobilization matrix rich in carboxylic functional groups essential for binding the progesterone-specific aptamer. Transmission electron microscopy (TEM) images of the NiO-Au nanocomposites revealed a highly porous structure composed of numerous nanoparticles, providing a large surface area and minimizing transport hindrance for subsequent catalytic reactions. The aptasensor demonstrated a dynamic concentration range spanning from 0.01 to 1000 nM, with an impressive detection limit of 1.86 pM. Furthermore, the proposed aptasensor was successfully employed for determining progesterone levels in human serum samples.<sup>145</sup>

A simple biosensor based on MIP was built by Laza *et al.* for the determination of progesterone in calf serum

samples.<sup>146</sup> Initially, AuNPs were electrochemically generated on GCE to enhance the surface activity. Subsequently, the MIP was deposited through the electropolymerization of aminophenol in the presence of the target analyte. The linear range and LOD values achieved with this platform were determined *via* SWV and found to be 0.2 to 125 nM and 0.17 nM, respectively. The biosensor's selectivity was evaluated against compounds with similar structures to progesterone, demonstrating no interference effects.<sup>146</sup>

**2.2.3 Saliva samples.** Saliva is gaining increasing recognition as an appealing diagnostic fluid for several reasons. Firstly, it contains various salivary biomarkers that accurately reflect both normal physiological states and disease conditions in humans. These biomarkers provide valuable insights into the health status of an individual. Secondly, saliva offers significant advantages over traditional blood sampling methods. Collecting saliva is non-invasive, painless, and relatively easy compared with venous blood collection. Additionally, saliva collection does not require highly trained medical personnel, specialized equipment, or strict storage conditions, reducing logistical challenges and costs associated with sample collection and transportation. Overall, the presence of disease-related biomarkers in saliva coupled with the ease of sample collection makes it a promising diagnostic fluid for a wide range of applications in healthcare and biomedical research.<sup>147</sup>

**2.2.3.1 Impedimetric biosensors.** The identification of testosterone in saliva has been accomplished, prompting studies into the reliability of salivary testosterone analysis. These studies aim to establish a strong correlation between salivary testosterone levels and serum testosterone concentration.<sup>148</sup>

Sun *et al.* developed an impedimetric immunosensor for testosterone monitoring in saliva samples.<sup>149</sup> In this work the self-assembled monolayer (SAM) of (3-aminopropyl)triethoxysilane (APTES) formed onto an indium tin oxide (ITO) glass electrode by immersion into APTES solution and then AuNPs were dropcast on the modified electrode. Finally, the plates were



washed and left to dry under  $N_2$  gas flow. The final step consisted of dropcasting a solution of Ab-testosterone for the immobilization of the antibody on the electrode thus obtaining the desired immunosensor (Ab-testosterone/AuNPs/APTES/ITO glass electrode). This developed sensor provided a linear concentration of testosterone from  $10 \text{ ng mL}^{-1}$  to  $0.5 \mu\text{g mL}^{-1}$ , with a limit of detection of  $3.9 \text{ ng mL}^{-1}$ .<sup>149</sup>

### 2.3 Insulin

The traditional electrochemical biosensors for insulin detection rely on the electroactivities of insulin due to the presence of electroactive amino acid residues, such as tyrosine, histidine, and cysteine, which are electro-active.<sup>150</sup> In the redox process insulin contains three disulfide bonds, the redox behaviour of which plays a crucial role in electrochemical detection.<sup>151,152</sup> Under electrochemical activation, these disulfide bonds can undergo reduction and oxidation processes, influencing the electrochemical properties. In electrochemical studies, insulin molecules adsorb onto the electrode surface, forming a monolayer. This adsorption allows for the reduction of disulfide linkages, resulting in the formation of thiol moieties. These thiol groups can undergo re-oxidation, leading to the reformation of the original disulfide bonds and release of electrons. Therefore, insulin is adsorbed onto the electrode surface, to which it transfers electrons due to the oxidation process, resulting in a measurable electrochemical signal. However, conventional bare electrodes are limited by slow response (*ca.* 100 s) due to slow electron transfer kinetics and the high potential required to electrocatalytically oxidize insulin.<sup>151</sup> Bare electrodes generally require high energy to induce electro-oxidation reaction of insulin, causing overpotential, a common problem found in electrochemical electrodes. Electrodes are rapidly deactivated resulting in the surface

fouling issue. This is caused by radical products of the disulfide oxidation process generated by anodic electrochemical reaction of insulin, which adsorb and accumulate on the electrode surface.<sup>153,154</sup> This therefore reduces the stability and lifetime of the electrodes. Because of the surface fouling issue, NPs have been incorporated into the electrodes to improve the efficiency and performance of electrochemical sensors. It is known that NPs with inherent catalytic activities can be used as electron transfer mediators or catalyzers to facilitate electron transfer at the interface between an electrode and insulin, leading to the reduction of voltage required for insulin oxidation, which could significantly prolong the lifetime of electrodes and increase electrochemical activities.

However, other interfering substances, such as uric acid, glucose, and ascorbic acid, in sample matrices are also electro-active and potentially influence electrochemical detection, causing false positive results.<sup>155</sup> Regarding specificity and selectivity of non-immune electrodes, biological insulin recognition molecules, such as antibodies, aptamers, and MIPs have been combined with NP-modified electrodes to allow insulin binding and prevent undesired compounds approaching the electrodes. However, the use of biological molecules requires appropriate storage conditions to prevent protein denaturation, with short lifetime of the modified electrodes.<sup>156</sup>

Table 4 summarizes the characteristics and performances of NP-based electrochemical biosensors for insulin in the literature.

**2.3.1 Serum samples.** Serum is the most used sample in diagnosis as it contains a high level of insulin. For this reason, most studies have selected insulin serum as the model for their tests in human samples.

**2.3.1.1 Voltammetric biosensors.** An electrochemical aptasensor based on a dual-signal strategy for detecting serum insulin

**Table 4** Electrochemical nanoparticle-based biosensors for insulin detection

Nanoparticles	Electrode	Receptor	Transducer	Body fluid	LOD	Linear range	Ref.
AuNPs	Gold electrode	Aptamer	SWV	Serum	0.1 pM ( $0.58 \text{ pg mL}^{-1}$ )	10 pM–10 nM	157
IONPs and rGO	MGCE	MIP	DPV	Serum	3 pM	0.01 nM–1 nM	158
AuNP@MoS <sub>2</sub> nanocomposites	GCE	Antibody	DPV	Serum	0.05 pM	0.1 pM–1 nM	159
Au@Cu <sub>5</sub> Zn <sub>8</sub> /HPCNC and AuNPs/NHG	GCE	Antibody	Amperometry	Serum	0.453 fg mL <sup>-1</sup>	0.022 pg mL <sup>-1</sup> –222 ng/mL	160
			DPV		0.341 fg mL <sup>-1</sup>	0.022 pg mL <sup>-1</sup> –11 ng mL <sup>-1</sup>	
			Chronoamperometry		0.0124 pg mL <sup>-1</sup>	0.1 pg mL <sup>-1</sup> –50 ng mL <sup>-1</sup>	
PdNP@MoS <sub>2</sub>	GCE	Antibody	Amperometry	Serum	0.52 pM	1.72 pM–17.2 nM	161
Zn <sub>2</sub> SiO <sub>4</sub> -PdNPs and AuINCs	GCE	Antibody	Chronoamperometry	Serum	0.25 fg mL <sup>-1</sup>	0.1 pg mL <sup>-1</sup>	162
			SWV		80 fg mL <sup>-1</sup>	–1 to 50 ng mL <sup>-1</sup>	
						0.1 pg mL <sup>-1</sup> –50 ng mL <sup>-1</sup>	
CQDs	GCE	Aptamer	EIS	Serum	106.8 pM	0.5 nM–10 nM	163
AgNFs-decorated rGO	ITO micro-disk electrode	Antibody	EIS	Serum	8.62 pM in buffer and 12.07 pM in serum	172.4 pM–172.4 nM	165
AuNPs	PGE	Aptamer	EIS	Plasma and urine	0.27 nM ( $1.57 \text{ ng mL}^{-1}$ )	1.0–1000.0 nM	168
Nano MIPs	Screen printed platinum electrodes	MIP	DPV	Plasma	26 fM	50–2000 pM	169
AuNPs	SPCE	Aptamer	SWV	Saliva	45 pM ( $0.26 \text{ ng mL}^{-1}$ )	0.05–15 nM	170



was developed and demonstrated.<sup>157</sup> Instead of directly measuring insulin oxidation, the assay utilized a combination of methylene blue (MB) and a redox reporter (Fc) to generate simultaneously detectable electrochemical signals. Additionally, AuNPs were employed as a catalyst. The preparation of the dual-probe aptasensor and its SWV response are shown in Fig. 10.

The gold electrode was modified with a “signal-off” probe (DNA1@MB-IBA) and a “signal-on” probe (DNA2Fc@GNPs/DNA1@MB-IBA) (Fig. 10A).

Redox activities were generated by Fc and MB for the “on” and “off” signals, respectively. In the absence of insulin, the MB probe was initially closer to the electrode than the Fc complex, allowing MB to effectively transfer electrons, resulting in a dominant off-signal observed at  $\sim 0.28$  V (Fig. 10B). Conversely, the on-signal of the Fc probe became more influential in the presence of insulin as the Fc complex approached the electrode, resulting in an enhanced oxidation peak at 0.38 V while decreasing that of the MB probe due to the displacement of the MB probe. AuNPs played a crucial role in mediating electron transfer to amplify electrochemical signal. In Fig. 10C, the SWV signal of the electrode without AuNP modification is displayed, and it points out an enhancement in the electrochemical response compared with the AuNP-modified electrode in Fig. 10B.

Due to the immobilization of aptamers, the aptasensor demonstrated high specificity for insulin, even in the presence

of interfering substances. When tested in insulin-spiked serum, the aptasensor showed analytical performance comparable to ELISA kits. Despite its high accuracy, sensitivity, and specificity for insulin determination, this dual-probe aptasensor is single-use and cannot be utilized for continuous measurement due to the immediate displacement of insulin upon insulin binding.

The specificity of electrochemical sensors toward insulin is one of the most important factors to be considered, as several blood components are electroactive. The employment of biomolecules certainly enables a high specific binding property; however, it may decrease the stability of the sensor, and needs special conditions for long-term storage. To overcome the limitations of using biorecognition molecules, researchers have recently integrated the MIP technique with the electrochemical sensor due to its high specificity, available multiple binding sites, and signal regeneration capability.

Despite the high targeting capability of immune-based electrochemical sensors for analytes, the stability of biorecognition molecules remains a major concern. To address this limitation, Zhu *et al.* demonstrated electromagnetic MIP (EMMIP) showing the use of magnetic NPs in electrochemical biosensors.<sup>158</sup> They prepared an insulin-MIP membrane using ternary  $\text{Fe}_3\text{O}_4$ @rGO/PANI NPs (MGP NPs).  $\text{Fe}_3\text{O}_4$  NPs were prepared on rGO sheets followed by polymerization of polyaniline (PANI) in the presence of insulin templates (Fig. 11).

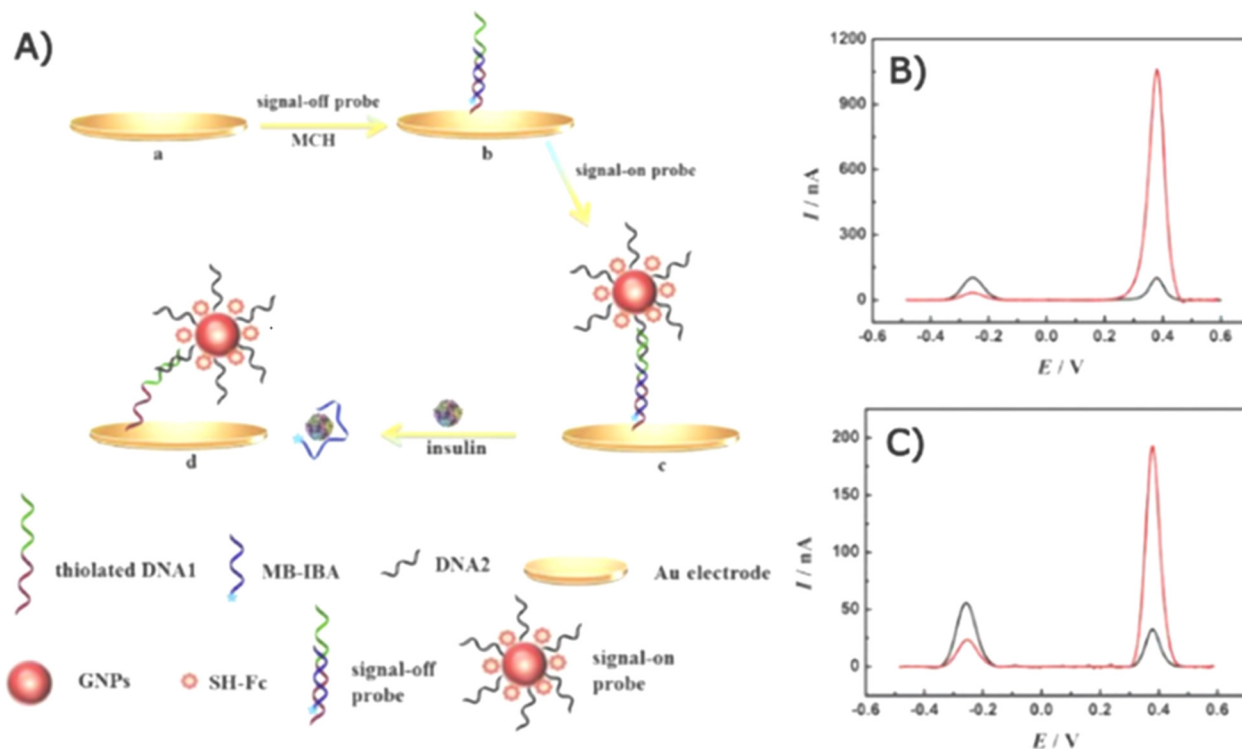


**Fig. 10** Schematics of a dual-probe electrochemical aptasensor. (A) Preparation of the Fc and MB probes on a gold electrode and the displacement of the MB probe upon the presence of insulin. The SWV response of the aptasensor (B) with and (C) without AuNP modification. The SWV response of the MB probe (“signal-off”) and the Fc probe (“signal-on”) at approximately 0.28 and 0.38 V, respectively. The black lines present the SWV response before insulin addition and the red lines present the SWV response after 100 pM insulin addition.<sup>157</sup>



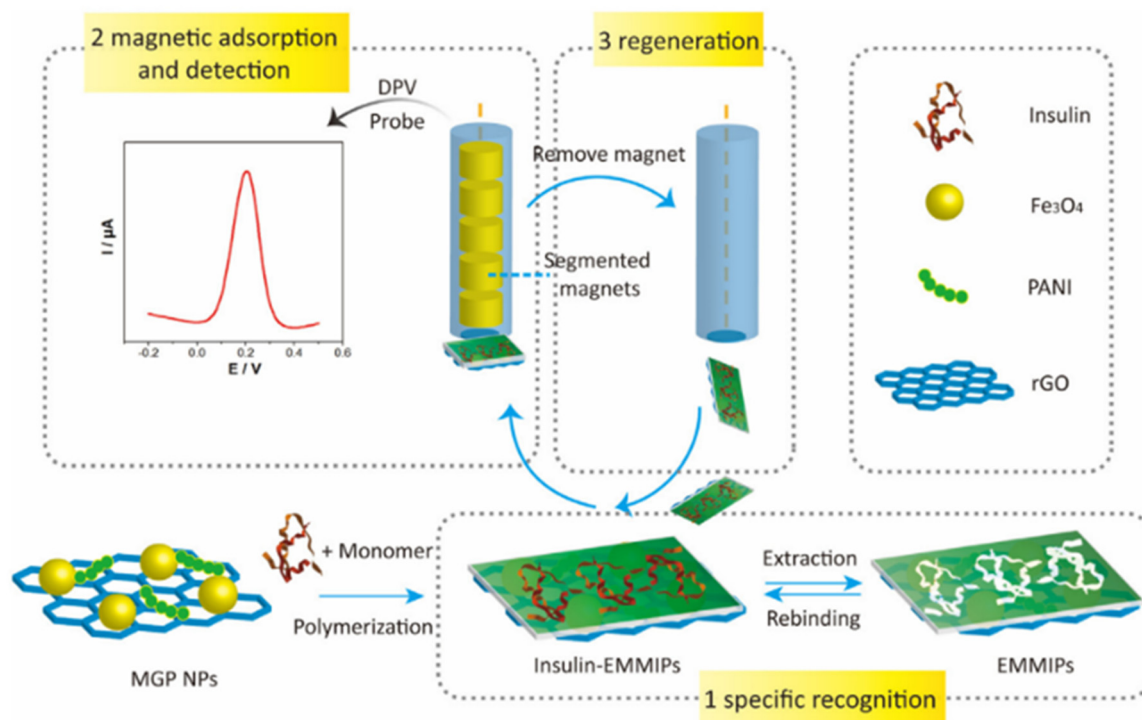


Fig. 11 Preparation and electrochemical detection operation of EMMIPs.<sup>158</sup>

This method exploited the unique characteristics of various materials to improve efficiency of electrochemical biosensors. PANI polymer and rGO are electrically conductive and influence electrocatalytic activity, promoting electron transfer at the interface. PANI was also used as an MIP membrane for insulin recognition. Unlike other studies, the role played by metallic NPs did not involve an enhancement of the electrochemical reaction, but the magnetic NPs were utilized to facilitate electrode regeneration.

Due to the embedding of  $\text{Fe}_3\text{O}_4$  NPs, the EMMIP membrane was responsive to the external magnetic force of a magnetic glassy carbon electrode (MGCE). Consequently, the MIP membrane was magnetically controllable. The adsorption of the EMMIP membrane could be controlled by applying or removing the external magnetic force of the MGCE.

Disadvantages of the conventional molecular imprinting technique include the degradation of protein during polymerization, such as exposure to high temperature, and it is difficult to imprint large and structurally complex molecules, which restricts their diffusivity. Surface imprinting is important as the imprinted sites are close to or at the surface of MIPs, avoiding the protein embedment in the polymer matrix, and thereby making the elution and rebinding of the target protein easier. It is superior to conventional imprinting process.

In conventional MIP electrodes, the electrode regeneration process is often complex and time-consuming. The EMMIP technique offers a convenient and rapid method for electrode regeneration by utilizing the magnetic properties of  $\text{Fe}_3\text{O}_4$

NPs. The EMMIP membrane preparation and insulin elution can be performed independently without the electrode, allowing for the removal of the EMMIP membrane and reloading of a fresh EMMIP membrane within 15–20 min under magnetic activation. This facilitates high-throughput analysis.

The study by Zhu *et al.* demonstrated the crucial role played by PANI in both insulin binding and electrochemical performance. Insufficient PANI loading resulted in reduced binding sites and a weaker electrochemical signal, while excessive PANI loading led to excessive crosslinking and hindered insulin template removal.

The EMMIP sensor exhibited good selectivity towards insulin in the presence of interfering substances and ions. The EMMIPs maintained their reusability for up to 10 times of insulin elution, adsorption, and measurement. Moreover, they could be stored for up to 20 d while retaining 90% of initial performance. The EMMIP assays showed a strong correlation with the results obtained from radioimmunoassays, validating their accuracy.

Overall, the EMMIP technique is a facile, simple, and convenient method for the sensitive and specific determination of insulin in complex serum samples. The magnetic properties of  $\text{Fe}_3\text{O}_4$  NPs enable rapid electrode regeneration and facilitate high-throughput analysis. The EMMIP sensor exhibits high sensitivity, selectivity, and reusability, making it a promising tool for insulin detection in clinical and research settings.

A sandwich-based electrochemical immunoassay for determining insulin was developed by Sun *et al.*<sup>159</sup> An enhancement of sensitivity was achieved using  $\text{MoS}_2$  nanosheets decorated



with AuNPs while its specificity was enabled by the immobilization of antibodies. The presence of MoS<sub>2</sub> nanosheets gave advantages of high specific surface area and excellent synergistic enhancement of the electrochemical response with metal NPs. AuNPs were *in situ* grown on MoS<sub>2</sub> nanosheets in their study. As a result, the nanocomposites were conductive and accelerated charge transfer at electrode surface. Furthermore, a hybridization chain reaction (HCR) was introduced to their immunoassay to further amplify electrochemical signal. The signalling molecules, RuHex, were electrostatically attached to DNA helices, resulting in 2.8-fold signal enhancement. This immunoassay showed good specificity, reproducibility, and stability. In the interference investigation, their immunoassay was selective to insulin, and other feasible molecules such as BSA, carcinoembryonic antigen (CEA), prostate-specific antigen (PSA), platelet-derived growth factor (PDGF) and vascular endothelial growth factor (VEGF) did not interfere with the detection. The immunosensor was stable for 2 weeks when stored at 4 °C. Moreover, the immunosensor could be used in a complex matrix of serum, showing recoveries between

96.0–106.4%, probably because of the presence of impurities in the sample. However, this method requires multiple steps which raise the complexity of the analysis.

Amperometry is also utilized among the voltammetric techniques. Each material presents unique advantages for enhancing electrochemical performance. Recent research has combined the strengths of various nanomaterials to achieve improved electrochemical detection of serum insulin.<sup>160</sup> One study involved the fabrication of nanocomposites: Au-adhered bimetallic Cu<sub>5</sub>Zn<sub>8</sub> hollow porous carbon nanocubes (Au@Cu<sub>5</sub>Zn<sub>8</sub>/HPCNC) and AuNP-deposited nitrogen-doped holey graphene (AuNPs/NHG), which were employed in a sandwiched immunoassay (Fig. 12).

The excellent performance of insulin detection was attributed to the synergy between the large electrocatalytically active area of Au@Cu<sub>5</sub>Zn<sub>8</sub>/HPCNC and the electrical conductivity of AuNPs/NHG. The bimetallic Cu<sub>5</sub>Zn<sub>8</sub> nanomaterials possessed inherent catalytic properties, making them excellent catalysts. When coupled with Au, they accelerated electron transfer at the GCE interface. Additionally, Cu<sub>5</sub>Zn<sub>8</sub>/HPCNC catalyzed the

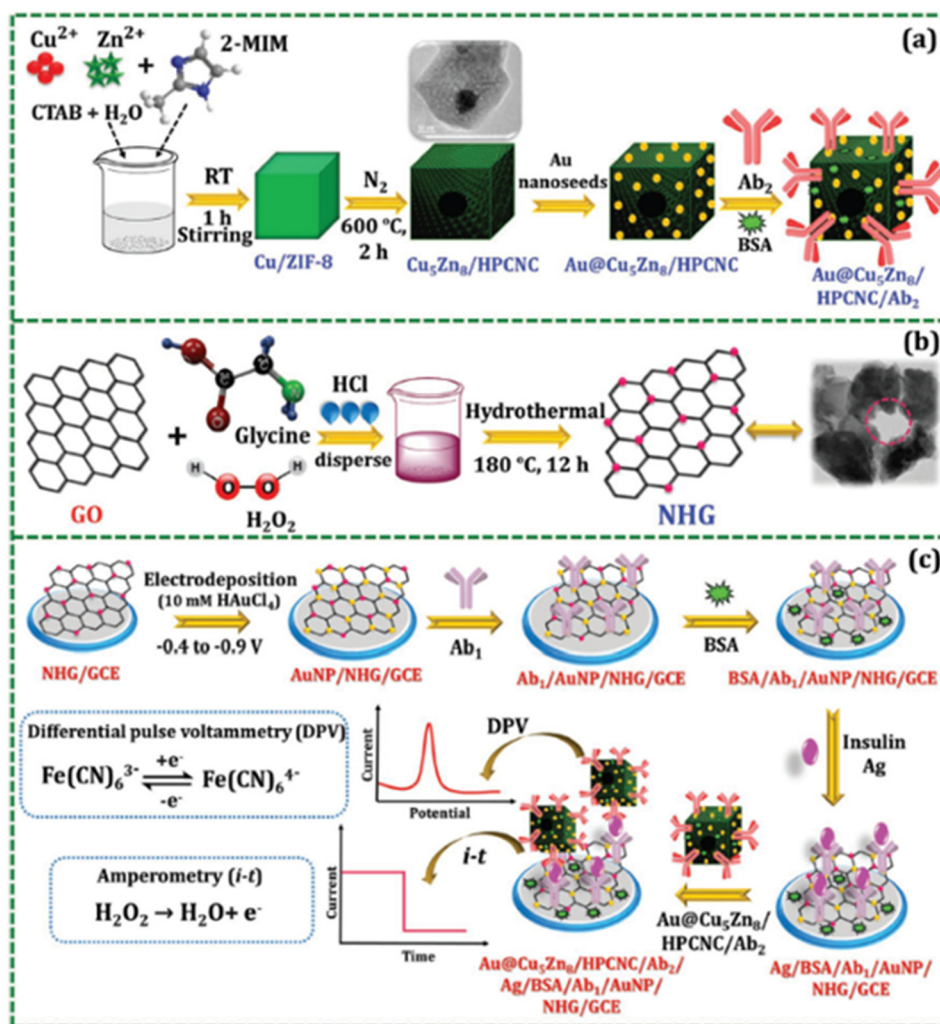


Fig. 12 Preparation of (A) Au@Cu<sub>5</sub>Zn<sub>8</sub>/HPCNC/Ab<sub>2</sub> and (B) NHG. (C) Preparation of immune-based electrochemical biosensors.<sup>160</sup>



reduction reaction of  $\text{H}_2\text{O}_2$  during amperometric measurements and enhanced the sensitivity of the DPV technique by speeding up electron transfer. Therefore, AuNPs/NHG enhanced electron transport while  $\text{Au@Cu}_5\text{Zn}_8/\text{HPCNC}$  acted as a signal amplifier, enabling more sensitive insulin detection.

The high conductivity and surface area of AuNPs/NHG, which contributed to accelerating electron transfer, were confirmed by CV and EIS in this study. No interference from other hormones, including leptin (LEP), ghrelin (GHRH), or other molecules such as dopamine (DA), BSA, or glucose (GLU), was observed.

Despite the incorporation of antibodies, the sensor exhibited good stability with 20 cycles of measurement and long-term storage of 11 d at 4 °C. The developed immunosensor was validated in human serum using electrochemical and ELISA techniques. The results obtained from these methods showed good correlation, indicating high reliability. Nonetheless, the total analysis time was 170 min, with 90 min for insulin binding and 80 min for AuNPs/NHG binding. Additionally, the efficiency of this immunosensor was temperature-dependent.

Another research group demonstrated the fabrication of an  $\text{H}_2\text{O}_2$ -based electrochemical immunosensor.<sup>161</sup> To improve analytical performance, the electrode was modified with PdNPs functionalized with  $\text{MoS}_x$  followed by antibody immobilization. Amorphous  $\text{MoS}_x$  provided a large surface area for the attachment of PdNPs and antibodies. The presence of PdNPs promoted catalysis of  $\text{H}_2\text{O}_2$  reduction *via* a synergistic effect leading to great current response enhancement. In terms of specificity, the immunosensor exhibited high specificity toward insulin in the presence of prostate specific antigen, IgG, and CEA. The electrode could perform for 60 cycles and the lifetime was 18 d. Moreover, the immunosensor was tested with insulin in a serum matrix, showing recoveries of 95.3–102.8%, suggesting high accuracy.

Development of the electrochemical enhancement technique related to metallic NPs was also demonstrated by Li *et al.* in 2018.<sup>162</sup> Their sandwich immunosensor was based on the use of PdNP-decorated zinc silicate spheres ( $\text{Zn}_2\text{SiO}_4$ -PdNPs) in the detection of insulin in human serum. This was a dual-function technique which was suitable for both SWV and chronoamperometric measurements, resulting in ultralow LOD.

Two NPs were included in their dual-function signal enhancement technique:  $\text{Zn}_2\text{SiO}_4$ -PdNPs and gold icosahedra nanocrystals (AuINCs).  $\text{Zn}_2\text{SiO}_4$ -PdNPs possessed excellent electrocatalytic properties toward  $\text{H}_2\text{O}_2$  reduction, thus improving the sensitivity of the chronoamperometry. In the meantime,  $\text{Zn}_2\text{SiO}_4$ -PdNPs hindered electron exchange at the electrode interface which, on the other hand, increased the current change and therefore positively affected the sensitivity of SWV detection. In case of AuINCs, they were introduced into the immunosensor for the immobilization of antibodies as they could attach with biomolecules tighter than the spherical shape.

The electrochemical signal exhibited maximized analytical efficiency at physiological pH, making the immunosensor in this study suitable for clinical applications. PSA, hepatitis B surface antigen (HBsAg), CEA and human serum albumin did not show significant electrochemical responses compared with the signals of insulin. After 2 weeks of storage, the signal of this dual-function assay reduced by 4.8%. The immunosensor was tested with insulin-spiked serum samples and exhibited good relative standard deviation (RSD) and recovery rate. Hence, selectivity and stability were acceptable while the LOD was extremely low with wide linear working range.

**2.3.1.2 Impedimetric biosensors.** A simple, cheap, and facile preparation to modify electrodes using carbon quantum dots (CQDs) was proposed by Abazar and Noorbakhsh.<sup>163</sup> CQDs were dispersed in a chitosan matrix to homogeneously distribute onto the electrode surface *via* electrostatic attraction. The CQD-chitosan nanocomposite offered feasibility for further biofunctionalization to enable selectivity toward insulin. Moreover, it was reported that CQDs were effective in preventing electrode fouling.<sup>164</sup> Insulin exposure led to a blocking effect because of structural conformation of the aptamer to bind insulin molecules. This resulted in an extreme increase in resistance using EIS measurement. Feasible interfering species including BSA, ascorbic acid, uric acid, and L-cysteine, did not affect insulin detection due to the presence of aptamers. The analytical performance of the impedimetric aptasensor developed in this study was investigated with serum samples and revealed recoveries of 96.8–105.6%, showing great accuracy. Moreover, in comparison with commercial methods, the developed CQD-chitosan based aptasensor showed recovery rates of 98.5–101.9%. The modified electrode could be kept at 4 °C for a week. However, as aptamer was used, the reaction was optimized at 60 min incubation.

Noble metallic silver nanoflowers (AgNFs) coupled with rGO nanocomposites were reported for the modification of electrodes for insulin detection.<sup>165</sup> Insulin molecules were recognized by antibody-immobilized AgNF-rGO on the electrode. Both AgNFs and rGO possessed excellent electrical conductivity. The presence of AgNFs increased the intensity and density of the electric field, making the nanocomposites more electrically conductive. Therefore, the synergistic effect between AgNFs and rGO resulted in significant acceleration of the electron transfer rate and therefore enhancement of the impedance response. The binding of insulin caused the increment of impedance which was proportional to insulin concentration. This impedimetric immunosensor was selective to insulin in the presence of C-reactive protein and BSA. The study noted the reusability, reproducibility, and stability (1 week) of the immunosensor.

**2.3.2 Plasma samples.** Beside human serum, a sufficient amount of insulin can be found in plasma samples for extraction for electrochemical quantification. Previous research suggests that there is no significant difference between the concentration of insulin in serum and plasma.<sup>166</sup> However, plasma insulin is more inconsistent than serum insulin, leading to lower reproducibility of results for insulin diagnosis.



sis.<sup>167</sup> Some research still focuses on the quantification of plasma insulin and will be discussed in this section.

**2.3.2.1 Impedimetric biosensors.** An immune-based electrochemical sensor integrating AuNPs and a conductive polymer was developed by Ensafi *et al.* for plasma insulin determination.<sup>168</sup> The surface of a pencil graphite electrode (PGE) was electrodeposited with a conductive poly-orthophenylene diamine polymer to enhance charge transfer and provide a porous structure for the attachment of AuNPs and insulin-recognizing aptamers. The successful fabrication resulted in a dramatic increase in insulin-electrode interaction and electrocatalytic activity. Attributed to the stability of the aptamers, the modified electrode retained acceptable electrochemical activity with up to 10 d of storage. Aptamers provided the modified electrode with the ability to recognize insulin. Nonetheless, the interaction between aptamers and insulin took 90 min to complete, possibly due to the slow binding kinetics of aptamers. Furthermore, a poly-orthophenylene diamine polymer was introduced to the PGE to increase analytical performance. However, it was found that the polymer coating could reduce specificity. Polymeric pores induced non-specific absorption of plasma proteins, as the electrooxidation of BSA, luteinizing hormone, and follicle-stimulating hormone was observed. The study pointed out the importance of optimizing the polymer thickness. Despite these limitations, the proposed electrode exhibited impressive outcomes with insulin-spiked plasma samples. The evaluation of this aptasensor with 50 nM and 70 nM insulin in plasma showed recoveries of 103% and 88.9%, respectively.

**2.3.2.2 Voltammetric biosensors.** The integration of biomolecules into electrochemical biosensors leads to the increase of logistical and storage costs. Although biomimetic MIP has been utilized in electrochemical biosensors, it has suffered with the complexity of biological samples, thus decreasing in reliability, and may not be practical for the clinical diagnosis of insulin. To address the challenge, Garcia Cruz *et al.* developed an electrochemical sensor using MIP nanoparticles (nanoMIPs) which was compatible with the complex matrix of serum.<sup>169</sup> The polymeric monomer formulation was computationally designed and then optimized in their research to achieve maximum sensitivity and selectivity for insulin determination.

Electroactive ferrocenylmethyl methacrylate monomer was presented in nanoMIP during fabrication as a redox probe. Hence, nanoMIPs provide insulin-capturing and signal-reporting activities. The recognition of insulin resulted in the change of electron transfer of ferrocene and a subsequent increase in current response, which was found to be proportional to insulin concentration. The nanoMIP-based electrochemical sensor developed in this study was highly robust as it could be kept for 168 d at 4 °C, showing extreme stability compared with the other reports mentioned earlier. In selectivity testing, it showed negligible response to potential interferences in blood including haemoglobin, human serum albumin, and human proinsulin C-peptide. According to this report, the nanoMIP-based electrochemical detection was

reproducible and accurate. Utilizing nanoMIPs offers several advantages such as high number of insulin-recognition sites, high stability, and high feasibility for clinical use. Moreover, the cost of production is lower than for other biomolecule-based sensors, making it more friendly for mass production at an industrial scale.

**2.3.3 Other biological fluids.** Blood is the predominant source of insulin, making it widely favoured for insulin detection in clinical settings. However, traditional blood-based insulin detection methods are invasive, requiring a small volume of blood to be drawn. Since insulin is not only available in the bloodstream, alternative body fluids, such as urine, sweat, and saliva, offer more non-invasive approaches for insulin detection. This section will discuss the use of alternative body fluids for insulin detection.

The use of urine as an alternative source for insulin detection offers several advantages over blood-based methods. Urine collection is non-invasive, painless, and can be performed multiple times throughout the day, allowing for continuous monitoring of insulin levels. Additionally, urine samples are less susceptible to interference from other proteins and compounds, potentially enhancing the accuracy of insulin detection.

The aptamer-based electrochemical sensor developed by Ensafi *et al.*, mentioned earlier in this review, also demonstrated the ability to identify insulin levels from urine samples.<sup>168</sup> Using the same PGE modification with AuNPs and poly-orthophenylene diamine polymer, EIS measurements revealed that the recovery rate for insulin determination in insulin-spiked urine (50–100 nM) was 93.0–94.0%. Other proteins did not interfere with the detection.

Nonetheless, urine-based insulin detection presents certain challenges. The concentration of insulin in urine is considerably lower than in blood, necessitating the development of more sensitive detection methods. Additionally, the presence of other metabolites and compounds in urine can potentially interfere with insulin detection.

The fabrication of a gold-modified aptasensor for insulin detection has been previously described. However, these methods typically rely on invasive blood collection. Recent efforts have demonstrated a promising non-invasive method to translate electrochemical insulin and glucose detection to a PoC device.<sup>170</sup> The authors demonstrated a miniaturized electrochemical assay for the prediction of prediabetes from saliva samples using a smartphone to facilitate home testing. An illustration of the configurative structure of the dual-marker aptasensor for insulin and glucose detection is shown in Fig. 13. AuNPs were chemically formed on the SPCE, followed by immobilization of MB-modified aptamers to simultaneously recognize insulin and glucose from the samples. This assembly was then integrated into a portable biochip for wireless analysis.

In the assay, the MB compound was responsible for generating redox activity, while AuNPs enhanced conductivity at the interface. Initially, the MB tags were positioned close to the sensing interface leading to substantial current responses for



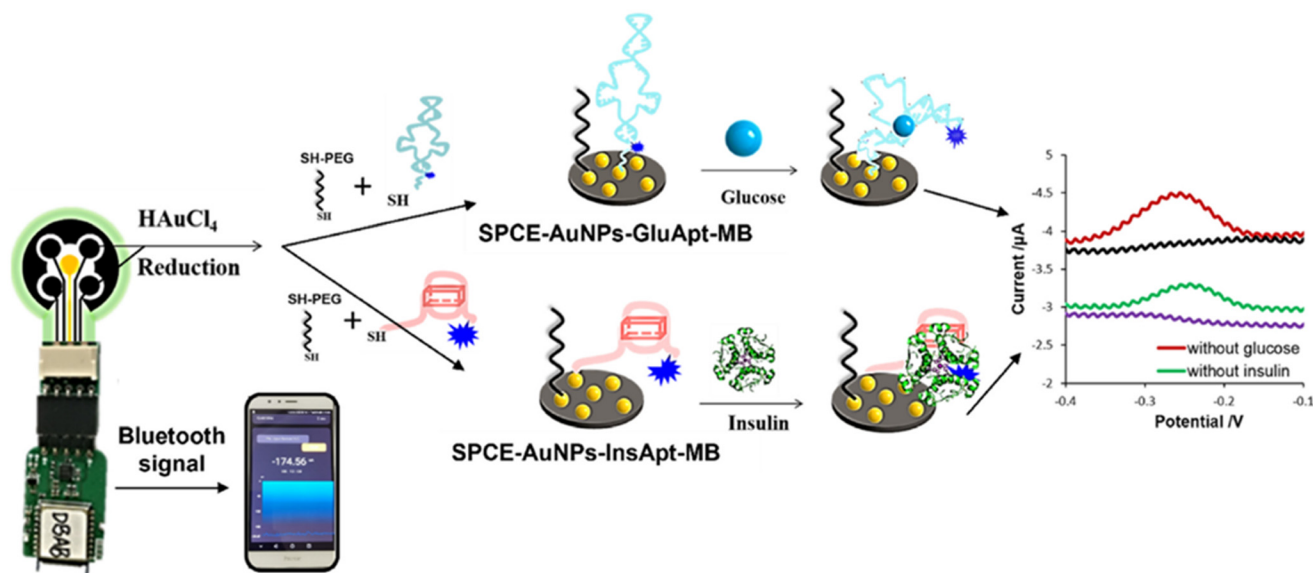


Fig. 13 Diagram of the simultaneous detection of insulin and glucose using the smartphone-assisted electrochemical aptasensor, measured by amperometric technique.<sup>170</sup>

both redox probes. The insulin- and glucose-aptamers responded to the presence of insulin and glucose by undergoing conformational changes that allowed them to capture these target compounds. The morphological alteration of the aptamers dislocated the MB tags farther away from the electrode surface, decreasing in the electrical currents of the corresponding channels.

The study not only presented the simultaneous detection capability and exceptional analytical efficiency of their aptasensor, but also exploited the switchable structure feature of the aptamers to enable real-time monitoring of these analytes. The reversibility of the current signal could be easily controlled by disrupting the G-quadruplex formation of the aptamers.<sup>171</sup>

Owing to the high specificity of engineered aptamers, particularly towards insulin and glucose, no cross-reaction between insulin-aptamers and glucose, or between glucose-aptamers and insulin, was observed. Moreover, human immunoglobulin (IgG), BSA, interferon- $\gamma$  (IFN- $\gamma$ ), and VEGF did not interfere with the detection of insulin and glucose. The modified aptasensor provided long-term storage of 30 d at 4 °C.

The feasibility of the portable aptasensor was evaluated with spiked saliva samples, demonstrating high reliability with recovery rates of 92.0–98.8% and 95.1–104.1% for insulin and glucose, respectively. Under optimization, the aptasensor required 30 min for antigen–aptamer interaction completion to maximize sensitivity. The operational period was shorter than that of the continuous monitoring MIP cryogel sensor (55 min)<sup>172</sup> and electrochemiluminescence (ECL) aptasensor (135 min).<sup>173</sup>

Overall, this aptasensor offered simple electrode preparation, continuous measurement, non-invasiveness, and feasibility for being a PoC device for predicting pre-diabetic progression.

## 2.4 Thyroid-stimulating hormone

Table 5 summarizes the characteristics and performances of nanoparticle-based EIS biosensors for TSH in the literature.

**2.4.1. Serum samples.** TSH is monitored in serum samples by electrochemical biosensors principally based on AuNPs combined with other chemical compounds to obtain highly sensitive platforms.

**2.4.1.1 Impedimetric biosensors.** Saxena *et al.* presented an immunosensor for the quantification of TSH by the EIS technique that showed a high sensitivity and selectivity of the sensor, with a LOD value of 0.001  $\mu\text{IU mL}^{-1}$  and a linear concentration range between 0.001 and 150  $\mu\text{IU mL}^{-1}$ .<sup>174</sup> A SPCE was functionalized by the addition of APTES that added free amino groups onto the surface of the electrode. After that, the electrode was further modified with AuNPs and cystamine dihydrochloride which bound with NPs and provided free amine groups. At the end, anti-TSH antibody was immobilized over the electrode with a direct immobilization. Thanks to EIS analysis it was possible to note a high affinity and selectivity for TSH molecule.<sup>174</sup>

In another work AuNPs were used to build a biosensor for TSH monitoring in serum samples by Beitollahi *et al.*<sup>175</sup> An ionic liquid/ carbon paste electrode (CILE) was modified with AuNPs and thioglycolic acid (TGA) that activated the surface of the electrode. After that, the thyroid-stimulating hormone immunosensor

Table 5 Electrochemical Au nanoparticle-based biosensors for TSH detection in the serum using antibody as receptor

Electrode	LOD	Linear range	Ref.
SPCE	0.001 $\mu\text{IU mL}^{-1}$	0.001–150 $\mu\text{IU mL}^{-1}$	174
CILE	0.1 $\text{ng mL}^{-1}$	0.2–90 $\text{ng mL}^{-1}$	175
Gold-SPE	—	—	176



was developed with the conjugation of TSH antibody by a covalent bond to the TGA/AuNPs/CILE platform. Before the measurement by EIS, the electrode was incubated with various concentrations of TSH and with horseradish peroxidase (HRP)-labeled TSH antibody. This TSH immunosensor showed a LOD of  $0.1 \text{ ng mL}^{-1}$  and the peak current growth with the increase in the concentration of TSH from  $0.2$  to  $90.0 \text{ ng mL}^{-1}$ .<sup>175</sup>

Saxena and colleagues proposed an impedimetric immunosensor based on AuNPs for TSH monitoring in serum samples.<sup>176</sup> Through EIS the concentration of TSH was detected by a novel immunosensor obtained by the modification of a gold SPE. Firstly, cysteamine hydrochloride was added onto a SPE; this was followed by the dropcast of colloidal AuNPs onto the functionalized working electrode. Cysteamine hydrochloride was added again onto the AuNP-modified electrode leading to AuNP-catalyzed amide bond formation with free amine groups on the platform. As a final step anti-TSH antibody was added to the built immunosensor. This work was based on the choice of the most suitable circuit used in EIS analysis for obtaining an EIS-based diagnostic device for TSH detection.<sup>176</sup>

## 2.5 Growth hormone

Table 6 summarizes the characteristics and performances of NP-based electrochemical biosensors for GH in the literature.

**2.5.1 Serum samples.** Because the concentration of growth hormone is very variable, and very low in the periods between pulses, analysis of the serum fraction of blood samples is a promising target for analysis for its relative concentration.

**2.5.1.1. Impedimetric biosensors.** For its sensitivity EIS is the most common technique used to detect the presence of growth hormone in serum. Two research groups, Rezaei B. *et al.* and Allafchian A. R. *et al.*, have developed two different types of NP-based electrochemical biosensors for the detection of growth hormone.<sup>177,178</sup>

Rezaei *et al.* described an electrode made of gold covered in AuNPs modified with 1,6-hexanedithiol (HDT) and functionalized with growth hormone-selective antibodies.<sup>177</sup>

Allafchian *et al.* utilized nanostructures of diphenylalanine deposited on the surface of GCE and modified with GH antibodies. When deposited and dried, diphenylalanine self-assembled in a flower-like structure approximately  $20 \mu\text{m}$  in diameter.<sup>178</sup>

The technique of EIS was also used to measure the quantity of GH that can be found in plasma, as reported by Bohlooli *et al.* in 2021. In their report Bohlooli *et al.* created an electrochemical biosensor based on a glass carbon electrode on which were deposited  $\text{Fe}_3\text{O}_4$  NPs; the electrode was then func-

tionalized with a layer of MIP (PANI) to detect the presence of growth hormone.<sup>179</sup>

**2.5.1.2 Voltammetric biosensors.** To find a solution to the challenge of studying the concentration of growth hormone in serum samples, different types of electrochemical biosensors based on NPs and exploiting different electrochemical analytical methods have been developed.

Serafin *et al.* in 2012 and later in 2014 developed two different types of NP-based electrochemical biosensors for the detection and quantification of GH in serum or saliva samples. In 2012 they developed a biosensor able to detect GH by SWV, and in 2014 they developed biosensors for the analysis of GH and prolactin by DPV in serum and saliva.<sup>89,180</sup> In 2012 they developed an electrochemical biosensor based on magnetic beads functionalized with anti-hGH (human growth hormone) antibodies; when in contact with GH the beads trapped the GH and became targets for the interaction with another aliquot of antibody molecules on which a third functionalized antibody was connected. The functionalization on the last antibody produced a signal when exposed to SWV, which was proportional to the amount of GH trapped by the magnetic beads. The magnetic properties of the beads were used to drive the nanoparticles with attached antibodies complex to the surface of the electrode.<sup>89</sup> In 2014 Serafin *et al.* realized an electrochemical biosensor based on a carbon printed electrode modified with carbon nanotubes on which was deposited a layer of poly(3,4-ethylenedioxythiophene) (PEDOT) NPs. On the surface of the modified electrode a layer of AuNPs was deposited and antibodies for hGH and prolactin were attached. In presence of either hGH or prolactin these electrodes could interact with dopamine, generating a detectable change on the peaks' shape of the DPV cycle.<sup>180</sup> This system was used to detect hGH and prolactin both in serum and in saliva with similar results.

## 3. Wearable biosensors for hormones detection

The development of comfortable, non-invasive biosensors to detect hormones in real time is becoming a real need. Real-time monitoring of hormones is possible with the development of wearable biosensors which allow their continuous detection in epidermal biofluids, such as ISF and sweat. Therefore, wearable biosensors technology has undergone great expansion in the last decade.<sup>181–185</sup> However, so far not many studies are available in this area.<sup>186–189</sup>

**Table 6** Electrochemical nanoparticle-based biosensors for GH detection

Nanoparticles	Electrode	Receptor	Transducer	Bodily fluid	LOD	Linear range	Ref.
AuNPs	Au	Anti-hGH	EIS	Serum	$93.0 \text{ fM}$	$135.6 \text{ fM} - 4.52 \text{ pM}$	177
Diphenylalanine nanoflowers	GCE	Anti-hGH	EIS	Serum	$17.2 \text{ fM}$	$4.52 \text{ fM} - 4.52 \text{ nM}$	178
$\text{Fe}_3\text{O}_4$	GCE	MIP	EIS	Plasma	$2.71 \text{ pM}$	$4.52 \text{ pM} - 4.52 \text{ nM}$	179
Magnetic beads	Au/CPE	Anti-hGH/hGH/Anti-hGH-labeled	SWV	Serum	$226 \text{ fM}$	$452 \text{ fM} - 4.52 \text{ nM}$	89
CNT/PEDOT NPs	CPE	Anti-hGH	DPV	Serum/saliva	$199 \text{ aM}$	$45.2 \text{ fM} - 45.2 \text{ nM}$	180



The main common issue to overcome in wearable device biosensors is the difficult electrode surface regeneration, which may cause poor reproducibility, thus affecting the possibility of continuous monitoring. Surface contamination, due to the accumulation of proteins and cells during continuous usage, may decrease the sensor sensitivity with consequent signal loss. Another issue is the use of nanomaterials, which is strictly dependent on their biocompatibility and biological cell safety. It is necessary that the NPs employed are totally biocompatible, as cytotoxicity could represent a severe hazard for clinical applications, due to the direct contact between the biosensor surface and the human skin.

Four works have been recently published in the literature regarding hormone detection with wearable devices.

In the first work, Mugo *et al.* developed a wearable textile electrochemical biosensor fabricated on a flexible cotton textile substrate, on which a layer of polyaniline decorated with carbon nanotubes and cellulose nanocrystals was deposited, to improve the electrical conductivity of the substrate. On this layer AuNPs and a MIP layer were formed and ensured selective capture of the cortisol molecule. With this set up Mugo *et al.* have achieved a LOD of 22.1 nM and a linear range between 27 nM and 136.6 nM in human sweat, with the biosensor being wearable as a patch and reusable for 15 measurements in a 30 d period. To ensure complete removal of cortisol in order to allow repeated measurement, 45 CV cycles were applied (−1.0–1.0 V range, 0.1 V s<sup>−1</sup> scan rate), and the phosphate buffer was replaced every 15 cycles.<sup>190</sup>

The integration of microfluidic technologies and wearable biosensors has also been utilized in laboratory medicine appli-

cations. A recent study by Lee and co-workers depicted a wearable lab-on-a-patch (LOP) platform comprising a stretchable, label-free, impedimetric biosensor and a stretchable microfluidic device for on-body non-invasive immunodetection of cortisol. This device utilized a 3D nanostructured Au working electrode and could detect cortisol in sweat at pM levels.<sup>191</sup>

Fiore *et al.* (Fig. 14) used a printed electrode modified with carbon black/Prussian blue NPs (CB/PB-NPs) as support for their electrochemical biosensor. On the printed electrode they deposited magnetic beads modified with a layer of antibodies supporting a layer of monoclonal cortisol antibodies, in order to have a functional distance between the beads and the antibody. The test devised by Fiore *et al.* works as a competitive assay, in which enough cortisol is modified with acetylcholinesterase to saturate the magnetic beads; in the presence of unmodified cortisol from a sweat sample, the marked cortisol is displaced and the signal generated by the system is reduced. With this system Fiore and collaborators reached an LOD of 8.3 nM and a linear range between 27.6 nM and 386.2 nM. Compared with the other biosensors in this section those of Fiore *et al.* are the least sensitive, but they are still sensitive enough to detect sweat cortisol levels of 8 ng mL<sup>−1</sup> to 140 ng mL<sup>−1</sup>; as a trade-off the result of the analysis can be read directly from a wearable patch on the patient using a NFC-capable smartphone and a dedicated app.<sup>192</sup>

There is only one paper regarding a wearable nanobiosensor for real-time oestradiol monitoring in sweat (Ye *et al.*). The device was based on aptamers appropriately attached to a MXene surface modified with AuNPs and bound to single-

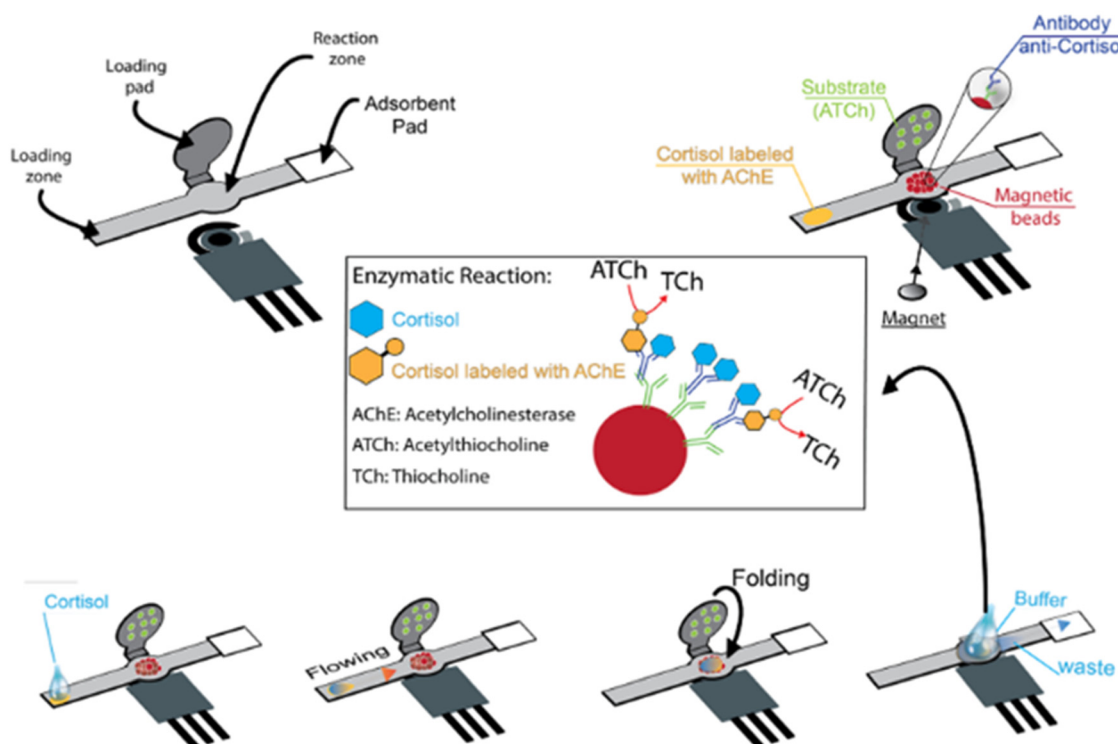


Fig. 14 Mechanism of action of an electrochemical biosensor with printed electrode modified with carbon black/Prussian blue nanoparticles.<sup>192</sup>



stranded DNA molecules tagged with a molecule that can directly donate or accept electrons under certain conditions. When an aptamer binds to an oestradiol molecule, it releases the redox molecule. That molecule is then recaptured by a nearby electrode, generating an electrical signal that correlates with the oestradiol level. The device was able to wirelessly transmit the data it collected to an app that runs on a smart phone, providing a simple interface for the users. Another innovation of this device was the design of the microfluidics that collected sweat and channelled it into the sensor. Tiny automatic valves incorporated in the microfluidics allowed only a small, fixed amount of sweat into the sensor and then prevented additional sweat from entering. The design enabled stable estradiol analysis without additional sweat disturbing the process. Moreover, to account for differences in sweat composition, the device also collected information about sweat pH, sweat salt levels, and skin temperature, and used it for real-time calibration. The biosensor offers extraordinary sensitivity with an ultra-low limit of detection of 0.14 pM.<sup>193</sup>

Despite the great research efforts made in several laboratories, the wearable devices developed in this field are still proofs-of-concept, and further research is still needed.

## 4. Conclusions and future perspectives

In this review, recent advances in NP-based biosensors for hormone detection are discussed, focusing on principles, techniques, and biological fluids of detection. Various electrochemical platforms and microfabrication techniques are described and compared, in order to improve the performance of biosensors, in terms of sensitivity, power output and reproducibility.

As shown in Tables 2–6, compared with the voltammetric biosensors reported for all hormones, the performance in terms of linear range and LOD of the reported impedimetric biosensors was weaker in these two aspects. Regarding the biological fluid of detection, all hormones have been detected in serum. Cortisol, insulin, testosterone, and GH were also determined in saliva, whereas urine was chosen in several works for sex hormone biosensor testing. It is interesting to note that TSH was detected only *via* EIS in serum samples, and that cortisol was the only hormone to be detected in human sweat, both with voltammetric and impedimetric transduction, but once again the voltammetric mode gave lower LODs, in the fempto-aptomolar range (Table 2).

The combination of biorecognition elements with innovative NPs holds much promise for enhancing hormone detection. However, there are still limitations and challenges to overcome for further application and commercialization.

Although NP-based biosensors for hormone detection are well developed, no commercially available device for PoC use exists yet, and the path towards commercialization of wearable technologies is even tougher.

Effectively, only very few start-up companies around the world have commercialized microneedle-based devices, like

Caura (UK) for simultaneous glucose and heart rate detection and Nutromics (Australia) for the continuous measurement of a range of micronutrients.

The main challenges for the development of microneedle-based platforms are the following: (i) the biofouling effect with consequent decrease of sensor reproducibility and lifetime; (ii) the low biocompatibility of the device, which can cause local skin inflammation; (iii) deficiencies in the calibration and validation protocols, which limit the accuracy of the device. Of course, the intense scientific work in this area shows great promise, but the major problem to overcome toward their possible marketization remains the gap existing between academic research and industry, together with the difficulties related to obtaining formal approvals for *in vivo* research studies. Moreover, the clinical significance of wearable testing data is another important issue which needs to be addressed.

However, it is very important to keep in mind that the successful realization of these challenging targets will be reached only by multidisciplinary work between electrochemistry, nano- and bio-engineering, electronics, and medical communities.

For the successful translation of “proof-of-concept” wearable biosensors into marketable PoC devices, an appropriate interface with smartphone-based wireless devices and algorithm-based applications has to be developed. At present, two technologies are used for real-time data streaming and analysis in wearable sensing devices: low-energy Bluetooth and NFC. Unfortunately, both of them have obvious drawbacks; for example, NFC needs to be close to the receiver electronics to work well. Therefore, a transmission system that achieves the ideal connection has yet to be developed. The integration of machine learning algorithms with smartphone-based sensors has the potential to lead to highly accurate analytical results.

In the near future, the development of all these technologies will be certainly scaled-up to the industrial level, and the amalgamation of hormone biosensors/wireless communication/data analysis platforms presents great potential for real-time remote health monitoring and personalized medicine development.

## Author contributions

NTKT and RA: conceptualisation, writing, editing, and review of the MS, FR wrote the sections about cortisol and GSH and created some of the images, TT wrote the sections about insulin, VG wrote the sections about sex hormones and TSH and created some images, CT wrote the introduction about the electrochemical biosensors, AI and AL reviewed the introduction section.

## Data availability

No primary research results, software or code have been included and no new data were generated or analysed as part of this review.



## Conflicts of interest

There are no conflicts to declare.

## Acknowledgements

This work was supported by the Italian Ministry of Education, Universities, and Research (Progetto PRIN 2022, No. 202285HFZY).

## References

- 1 N. Haroon and K. J. Stine, *Coatings*, 2023, **13**, 2040.
- 2 T. Zhang, X. Du and Z. Zhang, *Front. Bioeng. Biotechnol.*, 2022, **10**, 993015.
- 3 E. O. Adegoke, M. S. Rahman, Y. J. Park, Y. J. Kim and M. G. Pang, *Int. J. Mol. Sci.*, 2021, **22**, 3939.
- 4 T. Ozgocer, S. Yildiz and C. Uçar, *J. Immunoassay Immunochem.*, 2017, **38**, 147–164.
- 5 H. Zhang, Z. Cui, B. Yang, D. Fang, Y. Liu and Z. Wang, *Sci. Total Environ.*, 2021, **773**, 145569.
- 6 J. O. Abdulsattar and G. M. Greenway, *J. Anal. Sci. Technol.*, 2019, **10**, 34.
- 7 I. R. Suhito, K. M. Koo and T. H. Kim, *Biomedicines*, 2020, **9**, 15.
- 8 K. Ghoshal, in *Advanced Sensor Technology*, ed. A. Barhoum and Z. Altintas, Elsevier, 2023, pp. 261–295, DOI: [10.1016/B978-0-323-90222-9.00012-1](https://doi.org/10.1016/B978-0-323-90222-9.00012-1).
- 9 E. B. Bahadır and M. K. Sezgentürk, *Biosens. Bioelectron.*, 2015, **68**, 62–71.
- 10 S. Campuzano, P. Yáñez-Sedeño and J. M. Pingarrón, *Sensors*, 2020, **20**, 5125.
- 11 A. Núñez-De La Mora, G. R. Bentley, O. A. Choudhury, D. A. Napolitano and R. T. Chatterton, *Am. J. Hum. Biol.*, 2008, **20**, 2–14.
- 12 N. Gavrilova and S. T. Lindau, *J. Gerontol., B: Psychol. Sci. Soc. Sci.*, 2009, **64**(Suppl 1), i94–105.
- 13 G. Maskarinec, F. Beckford, Y. Morimoto, A. A. Franke and F. Z. Stanczyk, *Biomarkers Med.*, 2015, **9**, 417–424.
- 14 J. D. Meeker, S. R. Ravi, D. B. Barr and R. Hauser, *Reprod. Toxicol.*, 2008, **25**, 184–191.
- 15 H. T. Depypere, S. Bolca, M. Bracke, J. Delanghe, F. Comhaire and P. Blondeel, *Maturitas*, 2015, **81**, 42–45.
- 16 G. Jasienska and M. Jasienski, *Am. J. Hum. Biol.*, 2008, **20**, 35–42.
- 17 B. Nagy, J. Szekeres-Barthó, G. L. Kovács, E. Sulyok, B. Farkas, Á. Várnagy, V. Vértés, K. Kovács and J. Bódis, *Int. J. Mol. Sci.*, 2021, **22**, 11039.
- 18 M. Oettel and A. K. Mukhopadhyay, *Aging Male*, 2004, **7**, 236–257.
- 19 J. Flegr, J. Lindová and P. Kodým, *Parasitology*, 2008, **135**, 427–431.
- 20 W. Futterweit, N. L. McNiven, R. Guerra-Garcia, N. Gibree, M. Drosdowsky, G. L. Siegel, L. J. Soffer, I. M. Rosenthal and R. I. Dorfman, *Steroids*, 1964, **4**, 137–145.
- 21 G. D. Braunstein, R. E. Reitz, A. Buch, D. Schnell and M. P. Caulfield, *J. Sex. Med.*, 2011, **8**, 2924–2934.
- 22 T. G. Travison, H. W. Vesper, E. Orwoll, F. Wu, J. M. Kaufman, Y. Wang, B. Lapauw, T. Fiers, A. M. Matsumoto and S. Bhasin, *J. Clin. Endocrinol. Metab.*, 2017, **102**, 1161–1173.
- 23 M. Zea, F. G. Bellagambi, H. B. Halima, N. Zine, N. Jaffrezic-Renault, R. Villa, G. Gabriel and A. Errachid, *TrAC, Trends Anal. Chem.*, 2020, **132**, 116058.
- 24 M. Stachowicz and A. Lebidzińska, *Eur. Food Res. Technol.*, 2016, **242**, 2001–2009.
- 25 O. Stojadinovic, K. A. Gordon, E. Lebrun and M. Tomic-Canic, *Adv. Text. Wound Care*, 2012, **1**, 29–35.
- 26 A. S. Z. Abidin, R. A. Rahim, M. K. Md Arshad, M. F. F. Nabilah, C. H. Voon, T. H. Tang and M. Citartan, *Sensors*, 2017, **17**, 1180.
- 27 Y. Zhang, Q. Lai, W. Chen, C. Zhang, L. Mo and Z. Liu, *Chemosensors*, 2023, **11**, 90.
- 28 T. Iqbal, A. Elahi, W. Wijns and A. Shahzad, *Health Sci. Rev.*, 2023, **6**, 100079.
- 29 P. Pearlmutter, G. DeRose, C. Samson, N. Linehan, Y. Cen, L. Begdache, D. Won and A. Koh, *Sci. Rep.*, 2020, **10**, 19050.
- 30 D. Gonzalez, D. Jacobsen, C. Ibar, C. Pavan, J. Monti, N. F. Machulsky, A. Balbi, A. Fritzler, J. Jamardo, E. M. Repetto, G. Berg and B. Fabre, *Sci. Rep.*, 2019, **9**, 8213.
- 31 J. Marcos, N. Renau, G. Casals, J. Segura, R. Ventura and O. J. Pozo, *Anal. Chim. Acta*, 2014, **812**, 92–104.
- 32 S. Pradhan, B. D. Nicholson, S. Albin, R. L. Heise and V. K. Yadavalli, *Biosens. Bioelectron.: X*, 2022, **12**, 100280.
- 33 M. Venugopal, S. K. Arya, G. Chornokur and S. Bhansali, *Sens. Actuators, A*, 2011, **172**, 154–160.
- 34 M. Jia, W. M. Chew, Y. Feinstein, P. Skeath and E. M. Sternberg, *Analyst*, 2016, **141**, 2053–2060.
- 35 H. Raff and J. M. Phillips, *J. Endocr. Soc.*, 2019, **3**, 1631–1640.
- 36 Beckman Coulter, Cortisol RIA KIT, December 2022, accessed: April 2024, [online], available: <https://www.demeditec.com/en/products/cortisol-ria-it1841/ifu-it1841-cortisol-ria-ce2797-01-12-22-e.pdf>.
- 37 C. E. Karachaliou, G. Koukouvinos, D. Goustouridis, I. Raptis, S. Kakabakos, P. Petrou and E. Livaniou, *Biosensors*, 2023, **13**, 285.
- 38 A. Boolani, D. Channaveerappa, E. J. Dupree, M. Jayathirtha, R. Aslebagh, S. Grobe, T. Wilkinson and C. C. Darie, *Adv. Exp. Med. Biol.*, 2019, **1140**, 649–664.
- 39 S. Khumngern and I. Jeerapan, *Anal. Bioanal. Chem.*, 2023, **415**, 3863–3877.
- 40 J. Y. Moon, M. H. Choi and J. Kim, *Endocr.-Relat. Cancer*, 2016, **23**, R455–R467.
- 41 L. Goedeke and C. Fernández-Hernando, *Cell. Mol. Life Sci.*, 2012, **69**, 915–930.



- 42 M. Alemany, *Int. J. Mol. Sci.*, 2022, **23**, 11952.
- 43 R. Lauretta, M. Sansone, A. Sansone, F. Romanelli and M. Appetecchia, *Int. J. Endocrinol.*, 2018, **2018**, 4847376.
- 44 I. W. Craig, E. Harper and C. S. Loat, *Ann. Hum. Genet.*, 2004, **68**, 269–284.
- 45 G. Baggio, A. Corsini, A. Floreani, S. Giannini and V. Zagonel, *Clin. Chem. Lab. Med.*, 2013, **51**, 713–727.
- 46 I. Barsoum and H. H. Yao, *Trends Endocrinol. Metab.*, 2006, **17**, 223–228.
- 47 W. E. Stumpf, *Experientia*, 1990, **46**, 13–25.
- 48 J. Cui, Y. Shen and R. Li, *Trends Mol. Med.*, 2013, **19**, 197–209.
- 49 M. L. Rao and H. Kölsch, *Psychoneuroendocrinology*, 2003, **28**, 83–96.
- 50 Y. Zhang, X. Xiao, X. M. Zhang, Z. Q. Zhao and Y. Q. Zhang, *J. Biol. Chem.*, 2012, **287**, 33268–33281.
- 51 S. Zárate, G. Jaita, J. Ferraris, G. Eijo, M. L. Magri, D. Pisera and A. Seilicovich, *PLoS One*, 2012, **7**, e41299.
- 52 M. Birkhäuser, *Arch. Gynecol. Obstet.*, 1996, **259**(Suppl 1), S74–S79.
- 53 A. Kotov, J. L. Falany, J. Wang and C. N. Falany, *J. Steroid Biochem. Mol. Biol.*, 1999, **68**, 137–144.
- 54 H. Guo, Y. Zhang, D. A. Brockman, W. Hahn, D. A. Bernlohr and X. Chen, *Endocrinology*, 2012, **153**, 1183–1193.
- 55 L. Kolatorova, J. Vitku, J. Suchopar, M. Hill and A. Parizek, *Int. J. Mol. Sci.*, 2022, **23**, 7989.
- 56 V. Henderson, *Climacteric*, 2018, **21**, 333–340.
- 57 I. Sundström-Poromaa, E. Comasco, R. Sumner and E. Luders, *Front. Neuroendocrinol.*, 2020, **59**, 100856.
- 58 Y. Zhang, M. Nadeau, F. Faucher, O. Lescelleur, S. Biron, M. Daris, C. Rhéaume, V. Luu-The and A. Tchernof, *Mol. Cell. Endocrinol.*, 2009, **298**, 76–83.
- 59 M. Rossato, A. Nogara, M. Merico, A. Ferlin and C. Foresta, *Steroids*, 1999, **64**, 168–175.
- 60 B. Stoffel-Wagner, *Eur. J. Endocrinol.*, 2001, **145**, 669–679.
- 61 R. N. Elzenaty, T. du Toit and C. E. Flück, *Best Pract. Res. Clin. Endocrinol. Metab.*, 2022, **36**, 101665.
- 62 T. W. Kelsey, L. Q. Li, R. T. Mitchell, A. Whelan, R. A. Anderson and W. H. Wallace, *PLoS One*, 2014, **9**, e109346.
- 63 F. Fanelli, F. Baronio, R. Ortolano, M. Mezzullo, A. Cassio, U. Pagotto and A. Balsamo, *Sex. Dev.*, 2018, **12**, 50–94.
- 64 A. E. Kulle, F. G. Riepe, D. Melchior, O. Hiort and P. M. Holterhus, *J. Clin. Endocrinol. Metab.*, 2010, **95**, 2399–2409.
- 65 H. A. Feldman, C. Longcope, C. A. Derby, C. B. Johannes, A. B. Araujo, A. D. Coviello, W. J. Bremner and J. B. McKinlay, *J. Clin. Endocrinol. Metab.*, 2002, **87**, 589–598.
- 66 S. Bhasin, J. P. Brito, G. R. Cunningham, F. J. Hayes, H. N. Hodis, A. M. Matsumoto, P. J. Snyder, R. S. Swerdloff, F. C. Wu and M. A. Yialamas, *J. Clin. Endocrinol. Metab.*, 2018, **103**, 1715–1744.
- 67 G. Casals, R. F. Costa, E. U. Rull, H. F. Escobar-Morreale, J. Argente, G. Sesmilo and B. Biagetti, *Journal*, 2023, **4**, 52–69.
- 68 Z. Liu, in *Cellular Endocrinology in Health and Disease*, ed. A. Ulloa-Aguirre and Y.-X. Tao, Academic Press, Boston, 2nd edn, 2021, pp. 315–331, DOI: [10.1016/B978-0-12-819801-8.00015-6](https://doi.org/10.1016/B978-0-12-819801-8.00015-6).
- 69 G. Litwack, in *Hormones*, ed. G. Litwack, Academic Press, 4th edn, 2022, pp. 123–157, DOI: [10.1016/B978-0-323-90262-5.00022-6](https://doi.org/10.1016/B978-0-323-90262-5.00022-6).
- 70 Q. Hua, *Protein Cell*, 2010, **1**, 537–551.
- 71 S. E. Kahn, *Diabetologia*, 2003, **46**, 3–19.
- 72 A. Katsarou, S. Gudbjörnsdottir, A. Rawshani, D. Dabelea, E. Bonifacio, B. J. Anderson, L. M. Jacobsen, D. A. Schatz and Å. Lernmark, *Nat. Rev. Dis. Primers*, 2017, **3**, 17016.
- 73 V. Ormazabal, S. Nair, O. Elfeky, C. Aguayo, C. Salomon and F. A. Zuñiga, *Cardiovasc. Diabetol.*, 2018, **17**, 122.
- 74 F. Aun, M. M. Meguid, J. S. Soeldner and N. A. Stolf, *Postgrad. Med. J.*, 1975, **51**, 622–626.
- 75 A. H. Rubenstein, C. Lowy, T. A. Welborn and T. R. Fraser, *Metabolism*, 1967, **16**, 234–244.
- 76 I. Spitz, A. Rubenstein, I. Bersohn, A. Wright and C. Lowy, *J. Lab. Clin. Med.*, 1970, **75**, 998–1005.
- 77 K. Lian, H. Feng, S. Liu, K. Wang, Q. Liu, L. Deng, G. Wang, Y. Chen and G. Liu, *Biosens. Bioelectron.*, 2022, **203**, 114029.
- 78 S. Gaillard and F. E. Wondisford, in *Clinical Management of Thyroid Disease*, ed. F. E. Wondisford and S. Radovick, W.B. Saunders, Philadelphia, 2009, pp. 81–101, DOI: [10.1016/B978-1-4160-4745-2.00007-9](https://doi.org/10.1016/B978-1-4160-4745-2.00007-9).
- 79 K. Yoshida, T. Sakurada, K. Kaise, N. Kaise, T. Nomura, Y. Itagaki, M. Yamamoto, S. Saito and K. Yoshinaga, *Endocrinol. Jpn.*, 1988, **35**, 733–739.
- 80 R. W. Flynn, S. R. Bonellie, R. T. Jung, T. M. MacDonald, A. D. Morris and G. P. Leese, *J. Clin. Endocrinol. Metab.*, 2010, **95**, 186–193.
- 81 S. B. Soh and T. C. Aw, *Ann. Lab. Med.*, 2019, **39**, 3–14.
- 82 S. Ranabir and K. Reetu, *Indian J. Endocrinol. Metab.*, 2011, **15**, 18–22.
- 83 M. Caputo, S. Pigni, E. Agosti, T. Daffara, A. Ferrero, N. Filigheddu and F. Prodham, *Cells*, 2021, **10**, 1376.
- 84 C. C. Chernecky and B. J. Berger, *Laboratory Tests and Diagnostic Procedures*, Elsevier Health Sciences, 2012.
- 85 J. J. Kopchick, D. E. Berryman, V. Puri, K. Y. Lee and J. O. L. Jorgensen, *Nat. Rev. Endocrinol.*, 2020, **16**, 135–146.
- 86 K. Berneis and U. Keller, *Baillieres Clin. Endocrinol. Metab.*, 1996, **10**, 337–352.
- 87 U. Kumar, *Int. J. Mol. Sci.*, 2023, **25**, 436.
- 88 J. Ayuk and M. C. Sheppard, *Postgrad. Med. J.*, 2006, **82**, 24–30.
- 89 V. Serafin, N. Úbeda, L. Agüí, P. Yáñez-Sedeño and J. M. Pingarrón, *Anal. Bioanal. Chem.*, 2012, **403**, 939–946.
- 90 L. Gough, L. M. Castell, R. Gatti and R. J. Godfrey, *Sports Med. Int. Open*, 2015, **2**, 30.
- 91 M. Bidlingmaier and P. U. Freda, *Growth. Horm. IGF Res.*, 2010, **20**, 19–25.
- 92 D. Liu, J. Wang, L. Wu, Y. Huang, Y. Zhang, M. Zhu, Y. Wang, Z. Zhu and C. Yang, *TrAC, Trends Anal. Chem.*, 2020, **122**, 115701.



- 93 A. Haleem, M. Javaid, R. P. Singh, R. Suman and S. Rab, *Sens. Int.*, 2021, **2**, 100100.
- 94 W. Wang and S. Gunasekaran, *TrAC, Trends Anal. Chem.*, 2020, **126**, 115841.
- 95 M. Lv, Y. Liu, J. Geng, X. Kou, Z. Xin and D. Yang, *Biosens. Bioelectron.*, 2018, **106**, 122–128.
- 96 C. I. L. Justino, A. C. Duarte and T. A. P. Rocha-Santos, *Sensors*, 2017, **17**, 2918.
- 97 S. U. Singh, S. Chatterjee, S. A. Lone, H.-H. Ho, K. Kaswan, K. Peringeth, A. Khan, Y.-W. Chiang, S. Lee and Z.-H. Lin, *Microchim. Acta*, 2022, **189**, 236.
- 98 B. Senf, W.-H. Yeo and J.-H. Kim, *Biosensors*, 2020, **10**, 127.
- 99 V. Naresh and N. Lee, *Sensors*, 2021, **21**, 1109.
- 100 M. B. Kulkarni, N. H. Ayachit and T. M. Aminabhavi, *Biosensors*, 2022, **12**, 543.
- 101 E. S. Williams and L. M. Silverman, in *Essential Concepts in Molecular Pathology*, ed. W. B. Coleman and G. J. Tsongalis, Academic Press, 2nd edn, 2020, pp. 549–562, DOI: [10.1016/B978-0-12-813257-9.00030-9](https://doi.org/10.1016/B978-0-12-813257-9.00030-9).
- 102 L. C. Lopes, A. Santos and P. R. Bueno, *Sens. Actuators Rep.*, 2022, **4**, 100087.
- 103 A. P. F. Turner, *Science*, 2000, **290**, 1315–1317.
- 104 J. P. Chambers, B. P. Arulanandam, L. L. Matta, A. Weis and J. J. Valdes, *Curr. Issues Mol. Biol.*, 2008, **10**, 1–12.
- 105 D. R. Thévenot, K. Toth, R. A. Durst and G. S. Wilson, *Biosens. Bioelectron.*, 2001, **16**, 121–131.
- 106 M. Ramya, P. S. Kumar, G. Rangasamy, V. U. Shankar, G. Rajesh, K. Nirmala, A. Saravanan and A. Krishnapandi, *Chemosphere*, 2022, **308**, 136416.
- 107 A. Curulli, *Molecules*, 2020, **25**, 5759.
- 108 I.-H. Cho, D. H. Kim and S. Park, *Biomater. Res.*, 2020, **24**, 6.
- 109 J. L. Hammond, N. Formisano, P. Estrela, S. Carrara and J. Tkac, *Essays Biochem.*, 2016, **60**, 69–80.
- 110 X. Liu, M. Hoene, X. Wang, P. Yin, H.-U. Häring, G. Xu and R. Lehmann, *Anal. Chim. Acta*, 2018, **1037**, 293–300.
- 111 J. Xu, Y. Fang and J. Chen, *Biosensors*, 2021, **11**, 245.
- 112 S. R. Corrie, J. W. Coffey, J. Islam, K. A. Markey and M. A. F. Kendall, *Analyst*, 2015, **140**, 4350–4364.
- 113 Z. Rezapoor-Fashtali, M. R. Ganjali and F. Faridbod, *Biosensors*, 2022, **12**, 720.
- 114 V. Sharma, T. K. Sharma and I. Kaur, *J. Appl. Electrochem.*, 2023, **53**, 1765–1776.
- 115 D. Duan, H. Lu, L. Li, Y. Ding and G. Ma, *Microchem. J.*, 2022, **175**, 107231.
- 116 J. Liu, N. Xu, H. Men, S. Li, Y. Lu, S. S. Low, X. Li, L. Zhu, C. Cheng, G. Xu and Q. Liu, *Sensors*, 2020, **20**, 1422.
- 117 A. Tolun and Z. Altintas, in *Advanced Sensor Technology*, ed. A. Barhoum and Z. Altintas, Elsevier, 2023, pp. 593–646, DOI: [10.1016/B978-0-323-90222-9.00004-2](https://doi.org/10.1016/B978-0-323-90222-9.00004-2).
- 118 G. Deffo, T. F. N. Tene, L. M. Dongmo, S. L. Zambou Jikeng and R. C. T. Temgoua, in *Encyclopedia of Solid-Liquid Interfaces*, ed. K. Wandelt and G. Bussetti, Elsevier, Oxford, 1st edn, 2024, pp. 409–417, DOI: [10.1016/B978-0-323-85669-0.00040-4](https://doi.org/10.1016/B978-0-323-85669-0.00040-4).
- 119 S. Yeasmin, B. Wu, Y. Liu, A. Ullah and L.-J. Cheng, *Biosens. Bioelectron.*, 2022, **206**, 114142.
- 120 B. Yang, H. Li, C. Nong, X. Li and S. Feng, *Anal. Biochem.*, 2023, **669**, 115117.
- 121 N. K. Bakirhan, B. Uslu and S. A. Ozkan, in *Nanostructures for Antimicrobial Therapy*, ed. A. Fica and A. M. Grumezescu, Elsevier, 2017, pp. 55–83, DOI: [10.1016/B978-0-323-46152-8.00003-2](https://doi.org/10.1016/B978-0-323-46152-8.00003-2).
- 122 C. Nong, B. Yang, X. Li, S. Feng and H. Cui, *Microchem. J.*, 2022, **179**, 107434.
- 123 P. K. Vabbina, A. Kaushik, N. Pokhrel, S. Bhansali and N. Pala, *Biosens. Bioelectron.*, 2015, **63**, 124–130.
- 124 L. Cantelli, W. J. Paschoalino, S. Kogikosky, T. M. Pessanha and L. T. Kubota, *Biosens. Bioelectron.: X*, 2022, **12**, 100228.
- 125 Q. Liu, W. Shi, L. Tian, M. Su, M. Jiang, J. Li, H. Gu and C. Yu, *Anal. Chim. Acta*, 2021, **1184**, 339010.
- 126 Z. Huang, H. Chen, H. Ye, Z. Chen, N. Jaffrezic-Renault and Z. Guo, *Biosens. Bioelectron.*, 2021, **190**, 113451.
- 127 M. Sekar, M. Pandiaraj, S. Bhansali, N. Ponpandian and C. Viswanathan, *Sci. Rep.*, 2019, **9**, 403.
- 128 Q. Zhou, P. Kannan, B. Natarajan, T. Maiyalagan, P. Subramanian, Z. Jiang and S. Mao, *Sens. Actuators, B*, 2020, **317**, 128134.
- 129 R. D. Munje, S. Muthukumar, A. P. Selvam and S. Prasad, *Sci. Rep.*, 2015, **5**, 14586.
- 130 A. Kaushik, A. Vasudev, S. K. Arya and S. Bhansali, *Biosens. Bioelectron.*, 2013, **50**, 35–41.
- 131 B. Sun, Y. Gou, Y. Ma, X. Zheng, R. Bai, A. A. A. Abdelmoaty and F. Hu, *Biosens. Bioelectron.*, 2017, **88**, 55–62.
- 132 X. Liu, R. Zhao, W. Mao, H. Feng, X. Liu and D. K. Y. Wong, *Analyst*, 2011, **136**, 5204–5210.
- 133 S. Sanli, H. Moulahoum, F. Ghorbanizamani, Z. P. Gumus and S. Timur, *ChemistrySelect*, 2020, **5**, 14911–14916.
- 134 K.-J. Huang, Y.-J. Liu and J.-Z. Zhang, *Microchim. Acta*, 2015, **182**, 409–417.
- 135 E. Povedano, F. H. Cincotto, C. Parrado, P. Díez, A. Sánchez, T. C. Canevari, S. A. S. Machado, J. M. Pingarrón and R. Villalonga, *Biosens. Bioelectron.*, 2017, **89**, 343–351.
- 136 K.-J. Huang, Y.-J. Liu, J.-Z. Zhang, J.-T. Cao and Y.-M. Liu, *Biosens. Bioelectron.*, 2015, **67**, 184–191.
- 137 F. H. Cincotto, G. Martínez-García, P. Yáñez-Sedeño, T. C. Canevari, S. A. S. Machado and J. M. Pingarrón, *Talanta*, 2016, **147**, 328–334.
- 138 M. Ghanbarzadeh, A. Ghaffarinejad and F. Shahdost-Fard, *Talanta*, 2024, **273**, 125927.
- 139 J. Radecki and H. Radecka, in *Handbook of Bioanalytics*, ed. B. Buszewski and I. Baranowska, Springer International Publishing, Cham, 2022, pp. 747–760, DOI: [10.1007/978-3-030-95660-8\\_34](https://doi.org/10.1007/978-3-030-95660-8_34).
- 140 X. Liu, K. Deng, H. Wang, C. Li, S. Zhang and H. Huang, *Microchim. Acta*, 2019, **186**, 347.
- 141 Y. Wang, J. Luo, J. Liu, X. Li, Z. Kong, H. Jin and X. Cai, *Biosens. Bioelectron.*, 2018, **107**, 47–53.
- 142 M. J. Monerris, F. J. Arévalo, H. Fernández, M. A. Zon and P. G. Molina, *Sens. Actuators, B*, 2015, **208**, 525–531.



- 143 T. Ming, Y. Wang, J. Luo, J. Liu, S. Sun, Y. Xing, G. Xiao, H. Jin and X. Cai, *ACS Sens.*, 2019, **4**, 3186–3194.
- 144 Z. Zhao, H. Chen, Y. Cheng, Z. Huang, X. Wei, J. Feng, J. Cheng, S. M. Mugo, N. Jaffrezic-Renault and Z. Guo, *Microchim. Acta*, 2022, **189**, 178.
- 145 H. A. Samie and M. Arvand, *Bioelectrochemistry*, 2020, **133**, 107489.
- 146 A. Laza, A. Godoy, S. Pereira, P. R. Aranda, G. A. Messina, C. D. Garcia, J. Raba and F. A. Bertolino, *Microchem. J.*, 2022, **183**, 108113.
- 147 R. S. Malon, S. Sadir, M. Balakrishnan and E. P. Córcoles, *BioMed Res. Int.*, 2014, **2014**, 962903.
- 148 E. Lerchbaum, V. Schwetz, A. Giuliani, T. R. Pieber and B. Obermayer-Pietsch, *Fertil. Steril.*, 2012, **98**, 1318–1325, e1311.
- 149 Z. Sun, Y. An, H. Li, H. Zhu and M. Lu, *Int. J. Electrochem. Sci.*, 2017, **12**, 11224–11234.
- 150 A. S. Mackay, R. J. Payne and L. R. Malins, *J. Am. Chem. Soc.*, 2022, **144**, 23–41.
- 151 M. T. Stankovich and A. J. Bard, *J. Electroanal. Chem. Interfacial Electrochem.*, 1977, **85**, 173–183.
- 152 J. J. B. Nevado, J. R. Flores and G. C. Peñalvo, *Fresenius' J. Anal. Chem.*, 1999, **364**, 753–757.
- 153 A. Salimi, A. Noorbakhash, E. Sharifi and A. Semnani, *Biosens. Bioelectron.*, 2008, **24**, 792–798.
- 154 A. Noorbakhash and A. I. K. Alnajjar, *Microchem. J.*, 2016, **129**, 310–317.
- 155 I. Šišoláková, J. Hovancová, R. Oriňáková, A. Oriňák, L. Trnková, I. Třísková, Z. Farka, M. Pastucha and J. Radoňák, *J. Electroanal. Chem.*, 2020, **860**, 113881.
- 156 J. Hovancová, I. Šišoláková, R. Oriňáková and A. Oriňák, *J. Solid State Electrochem.*, 2017, **21**, 2147–2166.
- 157 Y. Zhao, Y. Xu, M. Zhang, J. Xiang, C. Deng and H. Wu, *Anal. Biochem.*, 2019, **573**, 30–36.
- 158 W. Zhu, L. Xu, C. Zhu, B. Li, H. Xiao, H. Jiang and X. Zhou, *Electrochim. Acta*, 2016, **218**, 91–100.
- 159 H. Sun, S. Wu, X. Zhou, M. Zhao, H. Wu, R. Luo and S. Ding, *Microchim. Acta*, 2018, **186**, 6.
- 160 R. Sakthivel, S. B. Prasanna, C.-L. Tseng, L.-Y. Lin, Y.-F. Duann, J.-H. He and R.-J. Chung, *Small*, 2022, **18**, 2202516.
- 161 Z. Gao, Y. Li, C. Zhang, S. Zhang, F. Li, P. Wang, H. Wang and Q. Wei, *Biosens. Bioelectron.*, 2019, **126**, 108–114.
- 162 Y. Li, L. Tian, L. Liu, M. S. Khan, G. Zhao, D. Fan, W. Cao and Q. Wei, *Talanta*, 2018, **179**, 420–425.
- 163 F. Abazar and A. Noorbakhash, *Sens. Actuators, B*, 2020, **304**, 127281.
- 164 F. Abazar, E. Sharifi and A. Noorbakhash, *Microchem. J.*, 2022, **180**, 107560.
- 165 A. K. Yagati, Y. Choi, J. Park, J.-W. Choi, H.-S. Jun and S. Cho, *Biosens. Bioelectron.*, 2016, **80**, 307–314.
- 166 J. M. Feldman and B. A. Chapman, *Clin. Chem.*, 1973, **19**, 1250–1254.
- 167 J. R. Henderson, *Lancet*, 1970, **296**, 545–547.
- 168 A. A. Ensafi, E. Khoddami and B. Rezaei, *Colloids Surf., B*, 2017, **159**, 47–53.
- 169 A. G. Cruz, I. Haq, T. Cowen, S. Di Masi, S. Trivedi, K. Alanazi, E. Piletska, A. Mujahid and S. A. Piletsky, *Biosens. Bioelectron.*, 2020, **169**, 112536.
- 170 S. Liu, Z. Shen, L. Deng and G. Liu, *Biosens. Bioelectron.*, 2022, **209**, 114251.
- 171 Y. Wu, B. Midinov and R. J. White, *ACS Sens.*, 2019, **4**, 498–503.
- 172 N. I. Wardani, T. Kangkamano, R. Wannapob, P. Kanatharana, P. Thavarungkul and W. Limbut, *Talanta*, 2023, **254**, 124137.
- 173 Y. Wang, H. Sha, H. Ke, X. Xiong and N. Jia, *Electrochim. Acta*, 2018, **290**, 90–97.
- 174 R. Saxena and S. Srivastava, *Mater. Today: Proc.*, 2019, **18**, 1351–1357.
- 175 H. Beitollahi, S. G. Ivary and M. Torkzadeh-Mahani, *Biosens. Bioelectron.*, 2018, **110**, 97–102.
- 176 R. Saxena and S. Srivastava, *Sens. Actuators, B*, 2019, **297**, 126780.
- 177 B. Rezaei, T. Khayamian, N. Majidi and H. Rahmani, *Biosens. Bioelectron.*, 2009, **25**, 395–399.
- 178 A. R. Allafchian, E. Moini and S. Z. Mirahmadi-Zare, *IEEE Sens. J.*, 2018, **18**, 8979–8985.
- 179 S. Bohlooli, S. Kia, S. Bohlooli and R. Sariri, *Monatsh. Chem.*, 2022, **153**, 39–48.
- 180 V. Serafin, G. Martínez-García, L. Agüí, P. Yáñez-Sedeño and J. M. Pingarrón, *Analyst*, 2014, **139**, 4556–4563.
- 181 J. Kim, A. S. Campbell, B. E.-F. de Ávila and J. Wang, *Nat. Biotechnol.*, 2019, **37**, 389–406.
- 182 J. Min, J. R. Sempionatto, H. Teymourian, J. Wang and W. Gao, *Biosens. Bioelectron.*, 2021, **172**, 112750.
- 183 A. Erdem, E. Eksin, H. Senturk, E. Yildiz and M. Maral, *TrAC, Trends Anal. Chem.*, 2024, **171**, 117510.
- 184 J. J. García-Guzmán, C. Pérez-Ràfols, M. Cuartero and G. A. Crespo, *TrAC, Trends Anal. Chem.*, 2021, **135**, 116148.
- 185 H. Sun, Y. Zheng, G. Shi, H. Haick and M. Zhang, *Small*, 2023, **19**, 2207539.
- 186 H. Teymourian, C. Moonla, F. Tehrani, E. Vargas, R. Aghavali, A. Barfidokht, T. Tangkuaram, P. P. Mercier, E. Dassau and J. Wang, *Anal. Chem.*, 2020, **92**, 2291–2300.
- 187 P. Bollella, S. Sharma, A. E. G. Cass and R. Antiochia, *Biosens. Bioelectron.*, 2019, **123**, 152–159.
- 188 P. Bollella, S. Sharma, A. E. G. Cass and R. Antiochia, *Electroanalysis*, 2019, **31**, 374–382.
- 189 P. Bollella, S. Sharma, A. E. G. Cass, F. Tasca and R. Antiochia, *Catalysts*, 2019, **9**, 580.
- 190 S. M. Mugo, W. Lu and S. Robertson, *Biosensors*, 2022, **12**, 854.
- 191 H.-B. Lee, M. Meeseepong, T. Q. Trung, B.-Y. Kim and N.-E. Lee, *Biosens. Bioelectron.*, 2020, **156**, 112133.
- 192 L. Fiore, V. Mazzaracchio, A. Serani, G. Fabiani, L. Fabiani, G. Volpe, D. Moscone, G. M. Bianco, C. Occhiuzzi, G. Marrocco and F. Arduini, *Sens. Actuators, B*, 2023, **379**, 133258.
- 193 C. Ye, M. Wang, J. Min, R. Y. Tay, H. Lukas, J. R. Sempionatto, J. Li, C. Xu and W. Gao, *Nat. Nanotechnol.*, 2024, **19**, 330–337.

